Article

Cell

Regulatory T Cell Specificity Directs Tolerance versus Allergy against Aeroantigens in Humans

Graphical Abstract

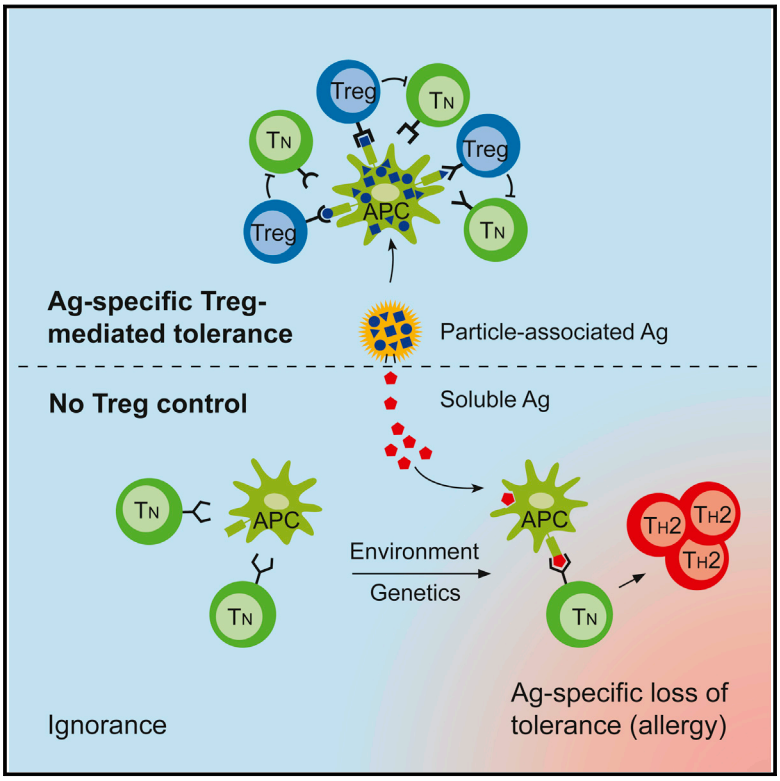

Authors

Petra Bacher, Frederik Heinrich, Ulrik Stervbo, ..., Michael Wallner, Margitta Worm, Alexander Scheffold

Correspondence

alexander.scheffold@charite.de

In Brief

Analyses of human blood identify T regulatory cells specific to aeroantigens, such as pollen, that are fully functional in allergic individuals, suggesting that it is the induction of Th2 responses and not Treg function per se that could be the underlying cause of allergy.

Highlights

- A comprehensive characterization of antigen-specific human Treg responses
- Harmless aeroantigens are major tolerogenic Treg targets
- Allergic patients have intact Treg responses against aeroantigens
- Th2 responses escape Treg control due to divergent antigen specificities

Data Resources

GSE77081

Bacher et al., 2016, Cell *167*, 1–12
November 3, 2016
http://dx.doi.org/10.1016/j.cell.2016.09.050

CellPress

Please cite this article in press as: Bacher et al., Regulatory T Cell Specificity Directs Tolerance versus Allergy against Aeroantigens in Humans, Cell (2016), http://dx.doi.org/10.1016/j.cell.2016.09.050

Regulatory T Cell Specificity Directs Tolerance versus Allergy against Aeroantigens in Humans

Petra Bacher,[1] Frederik Heinrich,[2] Ulrik Stervbo,[3,5] Mikalai Nienen,[3] Marco Vahldieck,[4] Christina Iwert,[5] Katrin Vogt,[5] Jutta Kollet,[4] Nina Babel,[3,5] Birgit Sawitzki,[5] Carsten Schwarz,[6] Stefan Bereswill,[7] Markus M. Heimesaat,[7] Guido Heine,[8] Gabriele Gadermaier,[9] Claudia Asam,[9] Mario Assenmacher,[4] Olaf Kniemeyer,[10] Axel A. Brakhage,[10] Fátima Ferreira,[9] Michael Wallner,[9] Margitta Worm,[8] and Alexander Scheffold[1,2,11,*]

[1]Department of Cellular Immunology, Clinic for Rheumatology and Clinical Immunology, Charité - University Medicine Berlin, 10117 Berlin, Germany

[2]German Rheumatism Research Centre (DRFZ) Berlin, Leibniz Association, 10117 Berlin, Germany

[3]Medical Clinic I, Marien Hospital Herne, Ruhr University Bochum, 44625 Herne, Germany

[4]Miltenyi Biotec GmbH, 51429 Bergisch Gladbach, Germany

[5]Berlin-Brandenburg Center for Regenerative Therapies, Institute of Medical Immunology, Charité - University Medicine Berlin, 13353 Berlin, Germany

[6]Department of Pediatric Pneumology and Immunology, Cystic Fibrosis Centre Berlin, Charité - University Medicine Berlin, 13353 Berlin, Germany

[7]Department of Microbiology and Hygiene, Charité - University Medicine Berlin, 10117 Berlin, Germany

[8]Department of Dermatology and Allergy, Allergy Center Charité, Charité - University Medicine Berlin, 10117 Berlin, Germany

[9]Department of Molecular Biology, University of Salzburg, 5020 Salzburg, Austria

[10]Department of Molecular and Applied Microbiology, Leibniz Institute for Natural Product Research and Infection Biology, Hans Knoell Institute (HKI), Jena and Friedrich Schiller University Jena, 07745 Jena, Germany

[11]Lead Contact

*Correspondence: alexander.scheffold@charite.de

http://dx.doi.org/10.1016/j.cell.2016.09.050

SUMMARY

FOXP3+ regulatory T cells (Tregs) maintain tolerance against self-antigens and innocuous environmental antigens. However, it is still unknown whether Treg-mediated tolerance is antigen specific and how Treg specificity contributes to the selective loss of tolerance, as observed in human immunopathologies such as allergies. Here, we used antigen-reactive T cell enrichment to identify antigen-specific human Tregs. We demonstrate dominant Treg-mediated tolerance against particulate aeroallergens, such as pollen, house dust mites, and fungal spores. Surprisingly, we found no evidence of functional impairment of Treg responses in allergic donors. Rather, major allergenic proteins, known to rapidly dissociate from inhaled allergenic particles, have a generally reduced capability to generate Treg responses. Most strikingly, in individual allergic donors, Th2 cells and Tregs always target disparate proteins. Thus, our data highlight the importance of Treg antigen-specificity for tolerance in humans and identify antigen-specific escape from Treg control as an important mechanism enabling antigen-specific loss of tolerance in human allergy.

INTRODUCTION

Specific antigen recognition is a hallmark of the adaptive immune response provided by antigen-specific B and T lymphocytes. Lymphocytes orchestrate a defense against pathogens, but they also actively maintain tolerance to self-antigens or innocuous exogenous antigens. FOXP3+ regulatory T cells (Tregs) represent a molecularly defined immunosuppressive T lymphocyte lineage that is essential for tolerance, as evidenced by the development of multi-organ autoimmunity in *FOXP3*-deficient humans and mice (Rudensky, 2011; Sakaguchi et al., 2008). Another hallmark of *FOXP3* deficiency or dysfunction is the neonatal development of severe allergies resulting from dysregulated T helper cell type 2 (Th2) responses (Barzaghi et al., 2012; Josefowicz et al., 2012; Kabat et al., 2016), demonstrating that Tregs are also required to maintain tolerance against innocuous environmental antigens at mucosal surfaces. Indeed, allergy development due to Treg instability (Kabat et al., 2016; Wan and Flavell, 2007) or defective Th2 regulation has been reported in mice (Jin et al., 2013; Joller et al., 2014; Ulges et al., 2015; Zheng et al., 2009) and is also discussed in human allergy (Ling et al., 2004).

However, in contrast to the broad neonatal allergies observed in *FOXP3*-deficient patients and mice, most allergic patients develop disease only against a limited number of allergenic proteins, whereas tolerance is maintained against the vast number of non-allergenic proteins contained in airborne particles, such as pollen, spores, or house dust mites. How such an antigen-specific loss of tolerance develops and, in particular, whether this is regulated via Treg antigen specificity is not understood. Indeed, human Treg target antigens relevant for mucosal tolerance are currently unknown (Gratz and Campbell, 2014). It has been demonstrated in mice that Treg specificity is biased toward the recognition of autoantigens (Hsieh et al., 2004; Kieback et al., 2016; Legoux et al., 2015; Malhotra et al., 2016) and that Tregs require continuous T cell receptor (TCR) stimulation, presumably

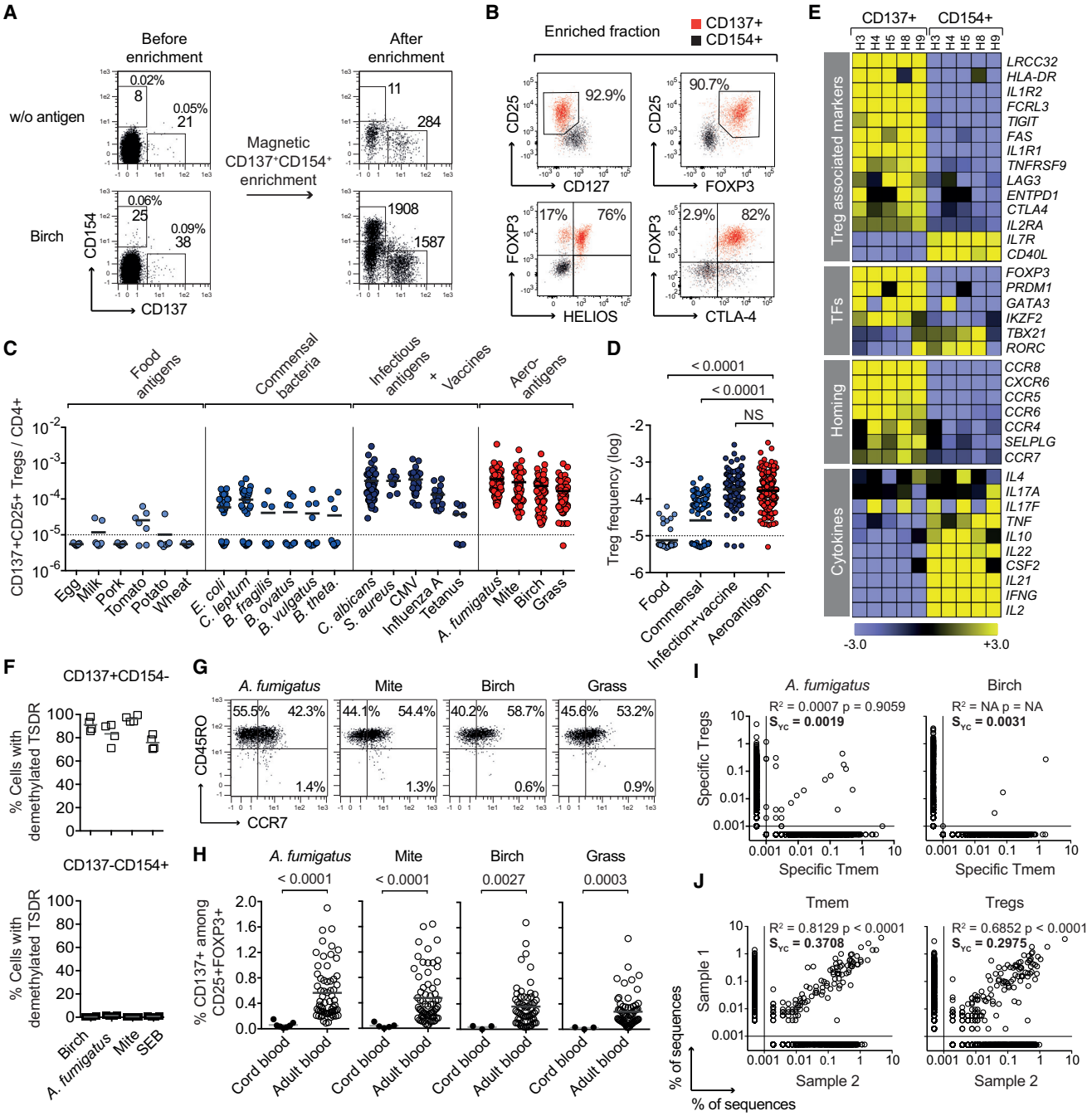

Figure 1. Tregs Specific for Aeroantigens Are Largely Expanded in Adult Blood

(A) Parallel detection of antigen-specific Tcons (CD154+) and Tregs (CD137+) with percentages among CD4+ and absolute cell counts.

(B) Overlayed flow-cytometric analysis of birch-specific CD154+ and CD137+ cells. Numbers indicate percentages among CD137+CD4+ T cells.

(C) Antigen-reactive CD137+ Treg frequencies within CD4+. Values below the detection limit (dashed line) were assigned arbitrary frequency values for graphical purposes (food: n = 7; commensal: *E. coli*, *C. leptum* n = 31, *B. ovatus* n = 8, others n = 10; *C. albicans* n = 67; CMV n = 32 [all seropositive]; influenza A n = 20; tetanus, *S.aureus* n = 8; aeroantigens n = 67).

(D) Treg frequencies were pooled and $\log_{10}$ transformed.

(E) Pairwise comparison of the $\log_2$-transformed gene expression values of *A. fumigatus*-reactive CD137+ Tregs and CD154+ Tcons (n = 5). TFs, transcription factors.

(F) Percentage of cells with demethylated *FOXP3* TSDR. Data are from four donors, two independent sorting experiments.

(G) Representative CD45RO and CCR7 staining of CD137+ Tregs.

(H) Antigen-reactive CD137+ Treg frequencies within total CD25+FOXP3+ Tregs (adult blood n = 67; cord blood *A. fumigatus* n = 7; mite n = 5; birch, grass n = 3).

(legend continued on next page)

by self-antigens, to suppress autoimmunity (Levine et al., 2014; Vahl et al., 2014). However, Tregs specific for exogenous antigens have been detected in naive (Moon et al., 2011; Zhao et al., 2011) and pathogen-infected mice (Shafiani et al., 2013; Suffia et al., 2006; Zhao et al., 2011) and humans (Bacher et al., 2014a; Ebinuma et al., 2008; Vukmanovic-Stejic et al., 2013). Furthermore, Tregs specific for commensal microbiota were found in murine intestinal tissues (Cebula et al., 2013; Lathrop et al., 2011), and murine Tregs against fetal antigens promote tolerance during pregnancy (Rowe et al., 2012; Samstein et al., 2012). This demonstrates that Tregs are not an exclusively self-reactive population. However, evidence for a dominant role of specific FOXP3+ Tregs in tolerance against aeroantigens is missing. Direct analysis of allergen-specific T cells from healthy and allergic patients revealed rather an altered balance of conventional T cell (Tcon) subsets, such as Th2 versus Th1 or interleukin (IL)-10-producing type-1 regulatory T cells (Tr1) (Meiler et al., 2008; Van Overtvelt et al., 2008; Wambre et al., 2012). So far, technical limitations have prevented the direct identification of antigen-specific Tregs in humans (Bacher and Scheffold, 2015). Therefore, it is presently unknown whether aeroantigens elicit antigen-specific Treg responses and how Treg antigen specificity versus Treg functionality impacts allergen-specific loss of tolerance in humans.

Here, we used a recently developed technology "antigen-reactive T cell enrichment" (ARTE) for a comprehensive characterization of human Treg responses against exogenous antigens to define the role of Treg antigen specificity for the regulation of mucosal tolerance.

RESULTS

High Frequencies of Antigen-Specific Tregs against Aeroantigens

So far, Treg antigen specificities in physiological repertoires have escaped detailed analysis due to the low frequency of individual clones and a lack of specific detection tools (Bacher and Scheffold, 2015). We recently overcame this difficulty by combining in vitro stimulation of human peripheral blood mononuclear cells (PBMCs) with antigens and subsequent magnetic enrichment of the rare antigen-activated T cells (antigen-reactive T cell enrichment, ARTE) (Bacher et al., 2013, 2014a). ARTE relies on the divergent expression of the activation markers CD137 (4-1BB) on Tregs and CD154 (CD40L) on Tcons after 7 hr of antigen activation (Figures 1A and 1B) (Bacher et al., 2014a; Schoenbrunn et al., 2012). Even complex antigens or undefined protein mixtures that are naturally processed by the autologous antigen-presenting cells (APCs) can be used for stimulation. However, variable abundance or processing of individual proteins may affect detection of certain specificities. Magnetic enrichment allows rapid processing of large cell samples (10^7–10^9) and thus the collection of a sufficiently large population of target cells for direct and in-depth characterization of antigen-specific Tcons and Tregs occurring at frequencies of 1 cell within 10^5–10^6 CD4+ T cells (Bacher et al., 2013, 2014a).

To identify physiological target antigens of human Tregs, we screened a panel of tolerogenic (food, commensal microbes, pollen) and immunogenic (infectious microbes, vaccines) candidate antigens for Treg versus Tcon reactivity using ARTE. Following 7 hr of stimulation with whole-antigen lysates, antigen-reactive Tregs (CD137+) and Tcons (CD154+) were isolated from $\geq 10^7$ PBMCs. Interestingly, we found considerable frequencies of Tregs (0.003%–0.29%, mean 0.030% within CD4+ T cells) against the human pathogens *Candida albicans*, *Staphylococcus aureus*, cytomegalovirus (CMV), and influenza A virus (Figure 1C). This demonstrates that pathogen-specific Tregs can be an inherent part of the physiological human pathogen-specific T cell response, which has been reported before for experimental infection models (Shafiani et al., 2013; Suffia et al., 2006; Zhao et al., 2011). Remarkably, we observed similarly high frequencies of antigen-specific Tregs against antigen lysates derived from innocuous environmental aeroantigens, such as plant pollen, house dust mites, or airborne fungi (*Aspergillus fumigatus*) (range 0.002%–0.34%, mean 0.026% within CD4+ T cells) (Figures 1C and 1D). By contrast, Tregs specific for other tolerogenic candidate antigens, such as food or commensal bacteria, were rare and/or highly variable among different donors. Treg identity was confirmed at the molecular and epigenetic level. Gene expression profiling of sorted *A. fumigatus*-specific CD137+ Tregs and CD154+ Tcons from five healthy donors (Figure 1E) revealed expression of Treg marker genes, such as *FOXP3*, *IL2RA* (CD25), *HELIOS*, *CTLA4*, *TIGIT*, *ENTPD1* (CD39), *GARP*, and a lack of *CD127* and *IL-2* as well as of effector cytokines. These results were confirmed at the protein level by flow-cytometric analysis (Figure 1B; Figure S1). In addition, >80% of the CD137+ Tregs showed a complete demethylation of the Treg-specific demethylated region (TSDR) at the *FOXP3* gene locus (Figure 1F), indicating a stable Treg phenotype (Baron et al., 2007).

Importantly, all aeroantigen-specific Tregs displayed a CD45RO+ memory phenotype (Figure 1G) and were absent in cord blood (Figure 1H), indicating their specific expansion in response to an antigen in the periphery. Individual T cells and their progeny can be identified via their unique T cell receptor (TCR) sequence. Thus, TCR sequence comparison based on next-generation sequencing allows the determination of clonal relations between certain subsets. TCR-β chain repertoire analysis of 10^4 fluorescence-activated cell-sorted (FACS) antigen-specific CD137+ Tregs revealed almost no overlapping TCRs with CD154+ memory Tcons (Tmems) (Figure 1I, similarity

(I and J) TCR-β sequence comparison of (I) antigen-specific Tmems versus Tregs and (J) duplicate-sorted *A. fumigatus*-specific Tmems and Tregs. Symbols outside the lines represent sequences found in one sample only. Linear regression and Yue-Clayton similarity index (S_{YC}) considering the proportion of each sequence in the respective sample are indicated (0 is total dissimilarity, 1 is identical populations). Data are representative of five (I) or two (J) donors from two independent sorting experiments.

Each symbol of (C), (D), (F), and (H) represents one donor. Horizontal bars indicate mean (C, D, F, and H). Statistical differences, one-way ANOVA with Tukey post hoc test (D), two-tailed unpaired Mann-Whitney test (H).

See also Figures S1, S2, and S3.

indices $S_{YC} < 0.01$), suggesting a unique repertoire of the aeroantigen-specific Tregs. For comparison, Figure 1J indicates the overlap between the respective duplicate-sorted antigen-specific Tregs ($S_{YC} = 0.29$) and Tmems ($S_{YC} = 0.37$).

Transcriptional profiling and flow-cytometric analysis revealed strong upregulation of the chemokine receptors *CCR4*, *CCR5*, *CCR6*, and *CXCR6* on aeroantigen-specific CD137+ Tregs, which have been reported to enable T cell migration to the lung tissue (Lee et al., 2011; Mikhak et al., 2013; Thomas et al., 2007) (Figure 1E; Figure S2). To confirm the specificity of the identified aeroantigen-reactive Tregs, sorted CD137+ Tregs and CD154+ Tcons were expanded and revealed high specificity following restimulation with their antigen in the presence of autologous APCs (Figures S3A–S3D). Treg cross-reactivity was detected between birch and grass pollen probably due to homologous proteins, as it was reported for Tcon responses before (Burastero et al., 2004). Furthermore, ex vivo CD154 and CD137 induction was inhibited by blocking antigen presentation via addition of an human leukocyte antigen (HLA)-DR antibody during stimulation with the antigen lysates (Figure S3E). Finally, in an in vitro functional assay, expanded antigen-specific CD137+ Tregs showed a strong antigen-specific suppressive capacity (Figure S3F).

Taken together, we identified considerable frequencies of clonally expanded Tregs with specificities for various exogenous antigens in human peripheral blood, which display all molecular, phenotypic, and functional features of stable Tregs. Remarkably, among the tolerogenic candidate antigens, particularly aeroantigens, elicited a strong Treg response, although we cannot exclude that food or commensal-specific Tregs are locally trapped within the intestinal tissues (Cebula et al., 2013; Lathrop et al., 2011) rather than circulating in peripheral blood. Overall, these data suggest that antigen uptake via the lungs is an important route for the induction of antigen-specific Treg responses in humans.

Tregs Specific for Aeroantigens Control Tcon Responses in Healthy Donors

To determine the overall T helper cell response for a given antigen, corresponding to states of tolerance or immunity, we next quantified the corresponding Tcon response in healthy donors. Tcons specific for pathogens displayed the expected memory and/or effector phenotype (Figure 2A) and occurred at higher frequencies than the corresponding Tregs (Figures S4A–S4D), resulting in a low Treg to Tmem ratio (Treg/Tmem ratio < 1) (Figures 2B and 2C). This supports the concept of a co-expansion of effector- and regulatory T cells during the immune reaction against pathogens to limit immunopathology. In stark contrast, a substantial fraction of aeroantigen-specific Tcons displayed a naive phenotype, as evidenced by a lack of CD45RO expression, but high expression of CCR7 (Figure 2A), CD45RA, CD27, and CD31 and lack of CD95, CD11a, and effector cytokine expression (Figures S4E–S4G). In concordance, the frequency of Tregs against aeroantigens clearly exceeded the frequency of the corresponding Tmem in the majority of donors (Treg/Tmem ratio > 1) (Figures 2B and 2C), indicating a dominant tolerogenic response. To corroborate this finding, we further dissected the antigen-specific Tmem compartment. TCR-β chain sequencing of sorted aeroantigen-specific (Birch) Tmems revealed no major clonal expansion, depicted by the overall high diversity (horizontal shape of the Rényi diversity profile; Figure 2D) and an even distribution of TCR-β sequences (low values of the Gini-coefficient) (Figure 2E). In contrast, oligoclonal expansions were present in the Tregs as well as in the pathogen-specific (*C. albicans*) Tmem compartment, indicated by the s-shaped Rényi profile (Figure 2D) and an increased Gini-coefficient (Figure 2E). Furthermore, in vitro-expanded aeroantigen-specific Tmem cells displayed 2–3 log lower functional avidity as compared to the corresponding Tregs (Figure 2F). Also, chemokine receptors relevant for lung homing, which were uniformly expressed by Tregs, were virtually absent on the corresponding Tmems (Figure S2).

Finally, we asked whether Tregs also dominate the in vivo response to antigen. Therefore, we analyzed ex vivo Ki-67 expression of birch-specific T cells to identify cells that have recently proliferated in vivo in the presence (within allergen season) and absence of in vivo antigen exposure (outside allergen season). Birch-specific Tregs revealed marginal proliferative activity outside the season (0.1%–8.5%, mean 5.6% from September to February) which increased (4.8%–20%, mean 11%) between March and May, indicating that these cells are actively dividing during the birch pollen season (Figure 2G). In contrast, for perennial *A. fumigatus* antigens, no seasonal influence on Ki-67 expression of specific Tregs was observed. Furthermore, in sharp contrast to birch-specific Tregs, Ki-67+ cells were absent among the birch- and *A. fumigatus*-specific Tcons at all times (Figure 2G).

Collectively, these data show that antigen-experienced, clonally expanded, and high-avidity-selected Tregs dominate the antigen-specific response against harmless environmental aeroantigens in humans. This strong Treg response seems to mark a true state of antigen-specific tolerance, since the corresponding Tcons lack the typical characteristics of in vivo antigen-primed effector and/or memory T cells and are indeed excluded from the immune response to antigen in vivo.

Tcons, but Not Tregs, Are Altered in Allergic Humans

Having identified Tregs as the major T cell population against aeroantigens, we analyzed whether antigen-specific Treg responses are quantitatively or qualitatively altered in allergic individuals, which could explain their failure to control allergy development. Birch-allergic donors were clearly distinguished from healthy individuals on the basis of increased Th2 cytokine production by birch-pollen-specific Tcons (Figures 3A and 3B), correlating with birch-specific immunoglobulin E (IgE) levels (Figures S5A and SB). Furthermore, birch-specific Tcons from allergic donors showed a significantly increased proportion and absolute number of Tmems (Figures 3C and 3D) as well as phenotypic markers of Th2 cells on a transcriptional and protein level (Figures 3E and 3F; Figures S5C and S5D) and lung homing chemokine receptor expression (Figure 3F). TCR-β chain repertoire analysis depicted oligoclonal expansion of birch-specific Tmems (Figure 3G), and Th2-derived cell clones showed 2–3 log higher functional avidity as compared to healthy donors (Figure 3H; Figures S5G and S5H). In summary, these data confirm a clear functional differentiation of birch-specific Tcons in allergic donors.

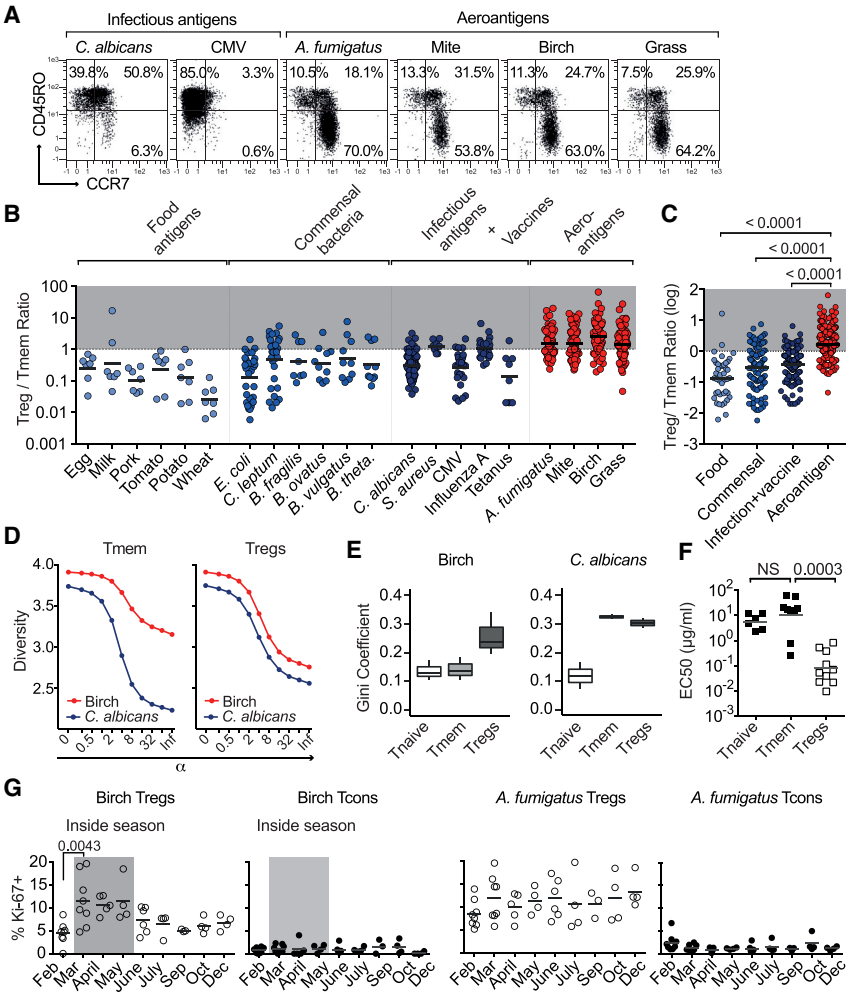

Figure 2. Tregs Dominate the Antigen-Specific Response to Aeroantigens in Healthy Donors

(A) Representative CD45RO and CCR7 staining of CD154+ Tcons.

(B) Ratio of antigen-specific Tregs/Tmems.

(C) Treg/Tmem ratios were pooled and $\log_{10}$ transformed.

(D and E) TCR-β sequence analysis of the top 50 expanded clones (birch n = 3, *C. albicans* n = 2).

(D) Rényi diversity profiles were calculated for pooled data. By varying the scaling parameter alpha, different diversity indices are calculated. At values of 0, 1, 2, and infinite the richness, Shannon diversity, Simpson diversity, and Berger-Parker index are calculated (see STAR Methods). This means that the sample with the highest value at $\alpha = 0$ has the highest richness, but the lower value at $\alpha =$ infinite indicates a higher proportion of the most abundant sequence, i.e. lower population diversity. A sample with a profile that is overall higher than the profiles of other samples is therefore more diverse, and an s-shaped versus a more horizontal curve shape indicates less evenness, i.e. more clonal expansion.

(E) Gini coefficient depicting the distribution of TCR-β sequences (0 is total equality, i.e., all clones have the same proportion, 1 is total inequality, i.e. a population dominated by a single clone).

(F) Expanded birch-specific cells were restimulated with increasing antigen concentrations. EC_{50} values were calculated from dose-response curves (naive T cells [Tnaive] n = 6; Tmems n = 9, Tregs n = 10; two to three independent experiments).

(G) Seasonal timeline of Ki-67 expression in healthy donors.

Each symbol in (B), (C), (F), and (G) represents one donor. Horizontal bars, geometric mean (B and F), mean (C and G). Statistical differences, one-way ANOVA with Tukey post hoc test (C and G), two-tailed unpaired Mann-Whitney test (F).

See also Figure S4.

However, in stark contrast, we did not observe any difference of the birch-specific Treg response in allergic versus healthy donors. Neither Treg frequencies (Figure 4A) nor the phenotypic Treg characteristics were affected (Figure 4B; Figures S5E and S5F). In vitro functional assays also confirmed the strong antigen-specific suppressive activity of expanded CD137+ Tregs from allergic donors (Figure 4C). We further observed no differences in the TCR-β chain repertoire (Figure 4D) or the functional avidity (Figure 4E) of the birch-specific Tregs between healthy versus allergic donors.

Thus, in allergic donors, antigen-specific Th2 responses develop despite the presence of a quantitatively and qualitatively normal Treg compartment, thereby decreasing the ratio of Tregs/Tmems to values ≤ 1 (Figure 4F). This escape of birch-specific Th2 cells from Treg-mediated control was also detected in vivo, because birch-specific Tmems from allergic donors displayed strongly increased Ki-67 expression during allergen season compared to healthy donors (Figure 4G). In addition, the frequencies of Ki-67+ birch-specific Tregs were also increased in allergic donors (Figure 4G), supporting that birch-specific Tregs are not functionally impaired per se. Changes in the Treg/Tmem ratio inside and outside the season were only observed in healthy donors (Figure S5I), demonstrating that, in allergic individuals, both populations are equally activated by the presence of antigen.

Tregs and Th2 Cells Target Different Proteins

Because Treg responses were not altered in allergic donors when whole protein extracts were used for stimulation, we hypothesized that the apparent lack of Treg-mediated Th2 control might be due to differing target antigens. Aeroantigens are typically inhaled as particles, such as intact pollen or fungal spores, containing multiple proteins (Platts-Mills and Woodfolk, 2011). However, the allergic response is mostly directed against very few immune-dominant allergens (Traidl-Hoffmann et al., 2009) (Figures S5J–S5L), whereas Treg targets are unknown. In contrast to the consistently high Treg responses against the whole protein extracts (Figure 1C), quantitation of Tregs specific for 24 individual proteins with different allergenic potential, derived from birch, grass, or *A. fumigatus*, revealed highly variable Treg responses in healthy donors (Figure 5A). Some proteins elicited detectable Treg responses in almost all analyzed

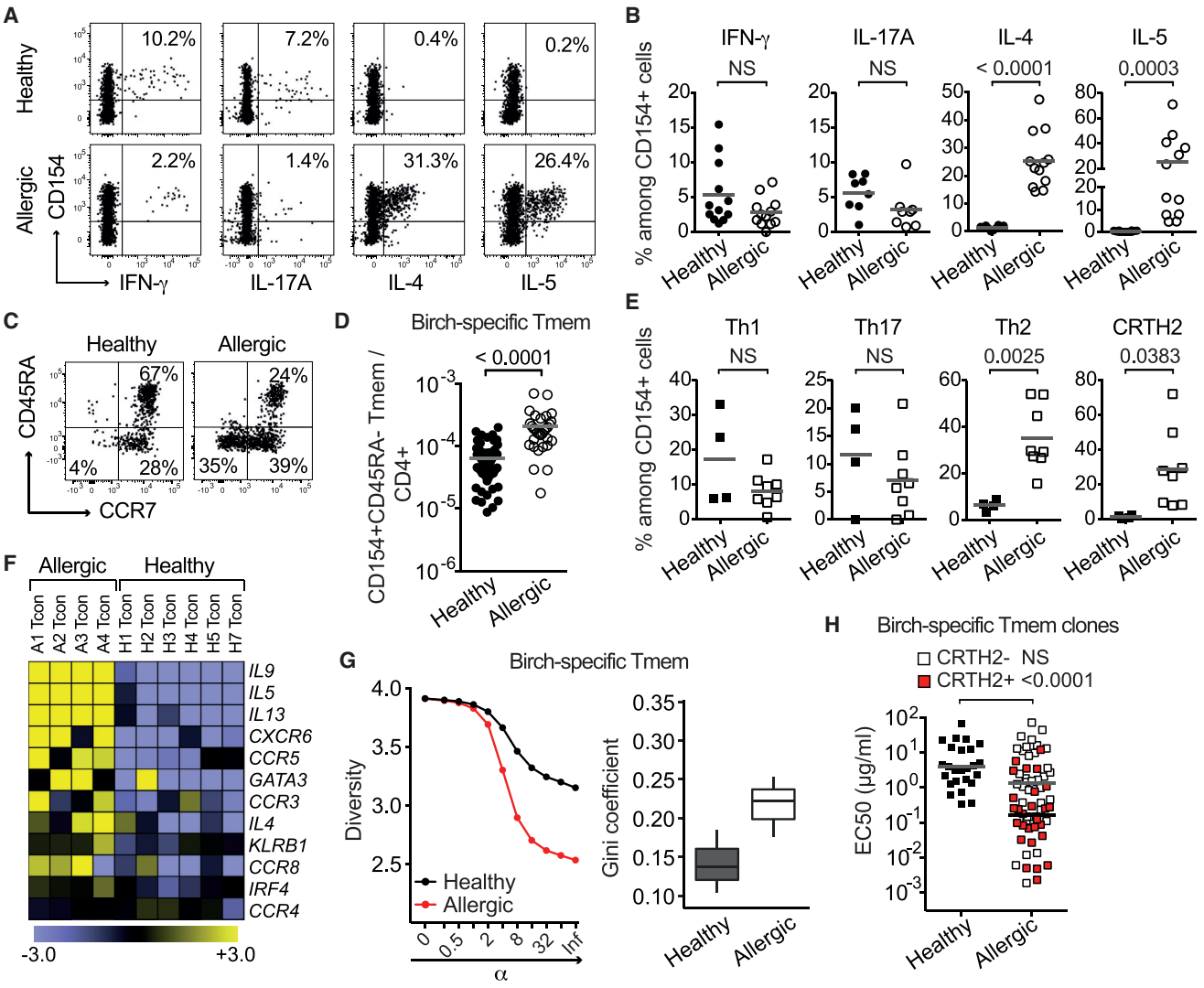

Figure 3. Functional Differentiation of Tcons Specific for Aeroantigens in Allergic Donors

(A and B) Ex vivo cytokine expression of birch-specific CD154+ Tcons (healthy, allergic n = 12, IL-17 n = 8; three to four independent experiments).

(C) Representative CD45RA and CCR7 staining of birch-reactive CD154+ Tcons.

(D) Birch-specific Tmem frequencies within CD4+ (healthy n = 60, allergic n = 30).

(E) Birch-specific CD154+ Tcons were classified according to chemokine receptor expression: Th1, CXCR3+; Th17, CXCR3−CCR6+CCR4+; Th2, CXCR3−CCR6−CCR4+ (healthy n = 4, allergic n = 8; two independent experiments).

(F) Log_2-transformed gene expression values of birch-specific CD154+ Tcons (healthy n = 6, allergic n = 4).

(G) TCR-β sequence analysis of the top 50 expanded clones of birch-specific Tmems. Rényi diversity profiles (left) and Gini coefficient (right) (healthy, allergic n = 3, two independent sorting experiments).

(H) Expanded birch-specific single cell clones were restimulated with increasing antigen concentrations. EC_{50} values calculated from dose-response curves from two healthy (n = 25) and two allergic donors (CRTH2+ n = 28; CRTH2− n = 37) are depicted.

Each symbol in (B), (D), and (E) represents one donor and (H) one T cell clone. Horizontal bars, mean (B, D, and E), geomean (H). Statistical differences, two-tailed unpaired t test (B and E), two-tailed unpaired Mann-Whitney test (D and H).

See also Figure S5.

donors, whereas others activated Tregs only in a subgroup of donors. However, in those donors with detectable Tregs against individual proteins, the frequencies of specific Tregs were in a similar range. These data suggest that, although all proteins can, in principle, induce Treg responses, they differ considerably in their Treg-activating potential, depicted as the percentage of healthy donors with detectable Tregs against that protein (Figure 5B). Interestingly, ranking proteins according to their Treg-activating potential revealed that known allergens (indicated in red in Figure 5B), including the major birch and grass allergens Bet v1, Phl p1, and Phl p5, possess rather low Treg response rates compared to minor allergens or non-allergenic proteins,

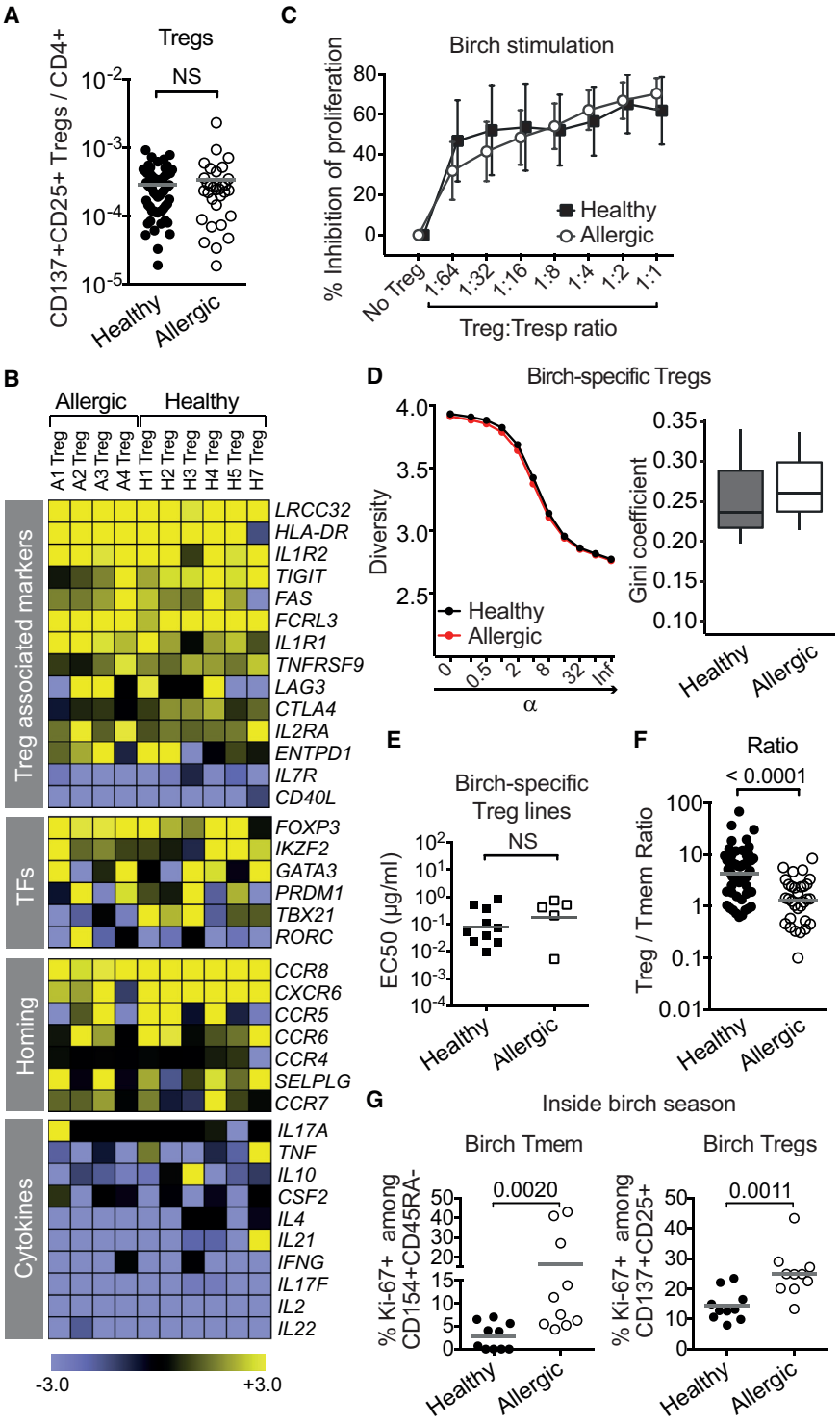

Figure 4. Tregs Specific for Aeroantigens Are Neither Quantitatively nor Qualitatively Altered in Allergic Donors

(A) Birch-specific Treg frequencies (healthy n = 60, allergic n = 30).

(B) Log_2-transformed gene expression values are depicted as pairwise comparison between birch-specific Tregs and Tcons (healthy n = 6, allergic n = 4). TFs, transcription factors.

(C) Inhibition of proliferation by expanded birch-specific Tregs after antigen-specific stimulation (healthy n = 4, allergic n = 5; mean ± SEM, two independent experiments).

(D) TCR-β sequence analysis of the top 50 expanded clones from CD137+ Tregs. Rényi diversity profiles (left) and Gini coefficient (right) (healthy, allergic n = 3; two independent sorting experiments).

(E) Expanded birch-specific Tregs were restimulated with increasing antigen concentrations. EC_{50} values were calculated from dose-response curves (healthy n = 10, allergic n = 5; three independent experiments).

(F) Ratio of birch-specific Tregs/Tmems (healthy n = 60, allergic n = 30).

(G) Ki-67 expression of birch-specific Tmems and Tregs inside birch pollen season (March to May) (healthy, allergic n = 10; two independent experiments).

Each symbol in (A) and (E)–(G) represents one donor. Horizontal bars, mean (A and G), geometric mean (E and F). Statistical differences, two-tailed unpaired Mann-Whitney test (A and E–G).

See also Figure S5.

which activate Tregs in the majority of donors. Importantly, the absence of specific Tregs does not lead to allergy per se, because several healthy donors also lack Tregs specific for nominal allergens as well as some other non-allergenic proteins, such as PST-1 or GliT. Thus, the absence of specific Tregs may provide a window of opportunity for subsequent Th2 development, which is prevented in the presence of Treg. To test this hypothesis of antigen-specific Treg-mediated protection from Th2 development, we directly analyzed whether Treg and Th2 responses against the same protein co-exists in individual healthy and allergic donors. Figure 5C shows the cumulative data from a cohort of healthy and allergic donors. Normalized frequencies of Th2 and Tregs against individual proteins from individual donors are plotted against each other (total data points n = 270). This side-by-side comparison indeed identifies a striking exclusivity of antigen-specific Treg versus Th2 responses. In fact, specific Th2 responses against a particular protein are only observed when Tregs reactive to the same protein are either completely lacking or their frequency is very low (Figure 5C). These data suggest that Tregs prevent development of Th2 responses in a highly antigen-specific manner and that the Treg-activating potential of an individual protein is a critical determinant of its allergenic potential.

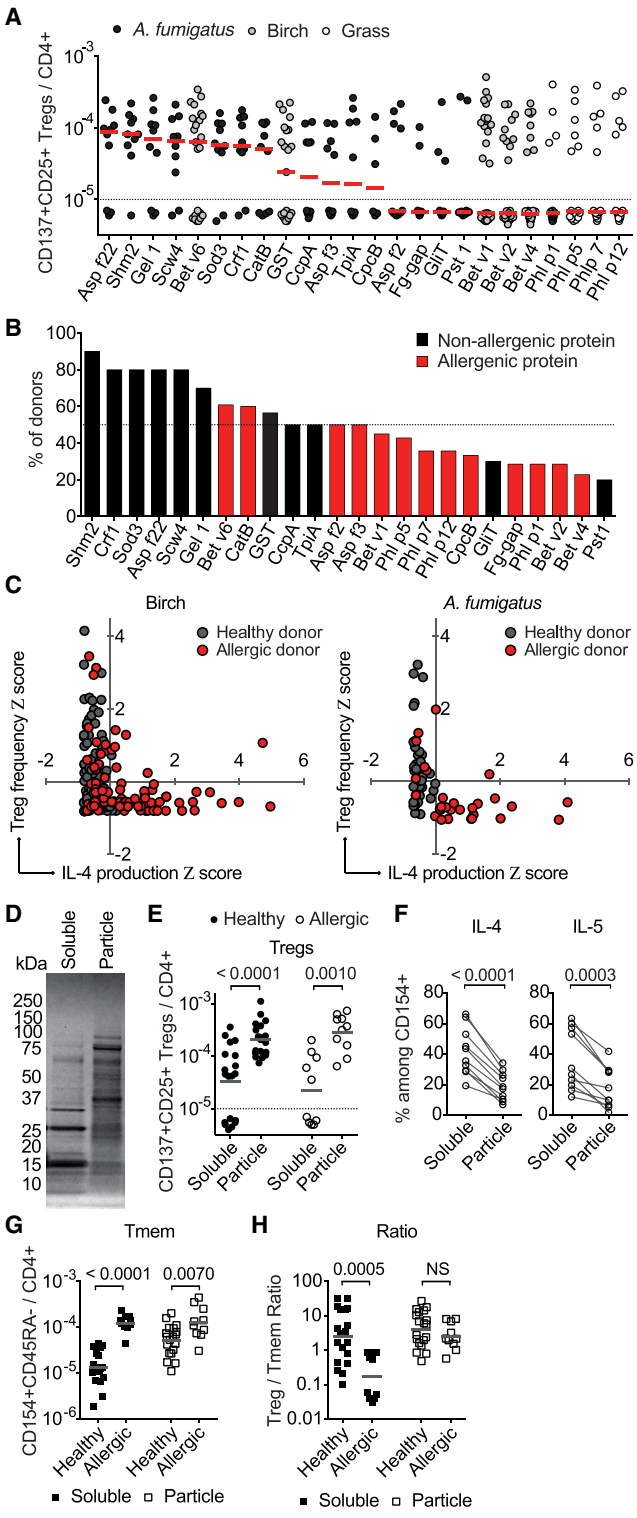

Figure 5. Tregs and Th2 Cells Do Not Share Antigenic Target Proteins

(A) Single protein-specific Treg frequencies in healthy donors. Values below the detection limit (dashed line) were assigned arbitrary frequency values for graphical purposes (*A. fumigatus*: CpcB, Fg-gap n = 7, others n = 10; Birch: Bet v1, v2, v4 n = 35; Bet v6, GST n = 23; Grass all n = 14).

Next, we wondered which protein characteristics impact the induction of Treg responses. To date, no unique allergen-defining feature has been identified, but, interestingly, all allergens are small (10–50 kDa), stable, and highly water-soluble proteins, resulting in their rapid release from airborne particles following uptake into the lung (Platts-Mills and Woodfolk, 2011). Such a physical separation of soluble and particle-associated antigens may lead to uptake by different antigen-presenting cells and eventually to different T cell responses. We therefore analyzed the Treg response against the particle-associated or soluble fractions of birch pollen. Crude extracts of soluble and particle-associated proteins were generated by 5 hr of water-incubation of birch pollen grains. The soluble protein fraction consisted primarily of small proteins as compared to the particle-associated fraction (Figure 5D). Strikingly, the particle-associated fraction generated strong and uniform Treg responses in all healthy and allergic donors (Figure 5E). In contrast, the Treg response against the soluble protein fraction was highly heterogeneous and significantly lower compared to the particle-associated fraction, reflecting the data obtained with the single proteins (Figure 5A). Th2 cytokine production in allergic donors was mainly observed in response to the soluble lysate (Figure 5F), confirming the presence of the dominant allergens. In line with that, the Tmem response against the soluble fraction strongly increased in allergic versus healthy donors (Figure 5G). The disparate targeting of individual proteins by Tregs versus Th2 cells for soluble, but not particle-associated, proteins in allergic donors is further illustrated by the strong and selective drop of the Treg/Tmem ratio against the soluble proteins (Figure 5H). These data suggest that particle-associated proteins effectively induce Treg responses and that these antigen-specific Tregs prevent Th2 and allergy development against particle-associated, but not soluble, proteins. In contrast, rapid protein dissociation from particles following uptake into the lung reduces the ability to induce Treg responses and conversely provides a window of opportunity for the development of Th2 responses and allergy.

(B) Percentage of donors with detectable single protein-specific Treg frequencies as determined in (A).

(C) *Z* score normalized frequencies of specific Tregs and Th2 cells (Birch: healthy, allergic n = 20, each symbol indicates frequencies of specific Tregs and Th2 cells for one protein [Bet v1, Bet v2, Bet v4, Bet v6, and GST] from one donor [total data points n = 200]; *A. fumigatus*: healthy n = 20, allergic n = 15, each symbol indicates frequencies of specific Tregs and Th2 cells against one protein pool [allergen pool, non-allergen pool, see also Figures S5J and S5K] from one donor, total data points n = 70).

(D) Birch pollen extracts analyzed by SDS-PAGE.

(E) Soluble and particle lysate-specific Treg frequencies (healthy n = 19, allergic n = 10; five independent experiments).

(F) Cytokine expression of soluble or particle lysate-stimulated CD154+ Tcons from allergic donors (n = 10).

(G) Soluble and particle lysate-specific Tmem frequencies (healthy n = 19, allergic n = 10).

(H) Ratio of birch-specific memory Tregs/Tmems (healthy n = 19, allergic n = 10).

Horizontal bars, median (A), geometric mean (E, G, and H). Statistical differences, two-tailed paired t test (E and F), two-tailed unpaired t test (G and H) of $\log_{10}$ transformed (E, G, and H), or linear (F) values.

See also Figure S5.

DISCUSSION

The antigen-specificity of human Tregs is still largely unknown, preventing analysis of fundamental aspects of Treg biology, such as antigen-specific tolerance, antigen-induced functional differentiation, and spatial distribution or memory. This limits our understanding of the role of Tregs for human immune pathologies and the development of Treg-based treatment strategies. The methodological approach introduced here provides a universal basis to directly address the aspect of Treg specificity in humans. Our work specifically highlights the role of antigen-specific Tregs for the regulation of tolerance versus allergy against aeroantigens.

The simultaneous quantification and characterization of antigen-specific Tregs and Tcons allows the study of their interplay and the definition of their mutual contributions to anti-pathogen immune responses as well as to states of active or passive tolerance. This led to the unexpected identification of a robust population of Tregs specific for innocuous aeroantigens that are present in all donors and feature molecular, phenotypic, and functional characteristics of peripherally expanded stable Tregs. Aeroantigen-specific Tregs seem to actively maintain tolerance, because a corresponding clonally expanded high-avidity-selected Tcon response was absent in healthy donors.

The identification of Tregs as dominant mediators of tolerance against aeroantigens is at odds with the current view of tolerance as a balanced Tcon response of protective IL-10/Tr1 versus pathogenic Th2 cells (Meiler et al., 2008; Van Overtvelt et al., 2008; Wambre et al., 2012). However, previous analyses have focused only on major allergenic proteins, whereas the large variety of non-allergenic proteins, which we identify here as main Treg targets, has been ignored. Indeed, major histocompatibility complex (MHC) multimers loaded with major Th2 target peptides have failed to identify dominant populations of allergen-specific Tregs in human blood (Palomares et al., 2011; Van Overtvelt et al., 2008; Wambre et al., 2012). In contrast, our finding of distinct protein specificities of Tregs versus Th2 cells in individual donors strongly suggests that if antigen-specific Treg responses are induced, they efficiently suppress Th2 development. In this way, Treg specificity would play a major role in restricting the repertoire of potential allergens to those proteins that fail to activate Treg responses. Together with the fact that Tregs from allergic donors were indistinguishable from healthy controls, these data also strongly argue against the idea of a generally impaired Treg response in allergic patients (Jin et al., 2013; Joller et al., 2014; Kabat et al., 2016; Ling et al., 2004; Soyer et al., 2013; Ulges et al., 2015; Wan and Flavell, 2007; Zheng et al., 2009). Although we cannot directly prove that human antigen-specific Tregs specifically suppress Th2 induction in humans, there is ample evidence from animal models for antigen-specific Th2 suppression by Tregs (Duan et al., 2011; Girtsman et al., 2010; Kearley et al., 2005). An alternative explanation to active Treg-mediated suppression would be that allergen-specific Tregs are selectively trapped in the respiratory tissues and are therefore not found in blood. However, we consider this unlikely, because Tregs against major allergens were present in the blood but were strictly absent in those allergic donors with detectable Th2 cells against the very same allergen (Figure 5C). Furthermore, recent studies in mice clearly show that Tregs with specificities for locally expressed model antigens are always detected in the periphery, despite local accumulation in tissues, including lung (Kieback et al., 2016; Legoux et al., 2015; Malhotra et al., 2016). Nevertheless, understanding the molecular and cellular details of Treg-mediated regulation in local tissues will be a major task for future studies.

Furthermore, our data reveal that allergens belong to a larger group of pollen- or spore-derived proteins, which have a generally diminished ability to induce Treg responses, resulting in a low incidence of antigen-specific Tregs against these proteins already in healthy donors. However, this also shows that the absence of specific Tregs does not lead to Th2 development per se. Instead, we propose that allergen-specific Th2 development is controlled at two independent checkpoints. The dominant immune reaction to inhaled preferentially particle-associated antigens is antigen-specific Treg-mediated tolerance. Antigens escaping this first checkpoint primarily seem to be ignored by the immune system, as suggested by the absence of clonally expanded antigen-specific Tcons in healthy donors. Proteins that fail to induce specific Treg responses but remain associated with the inhaled particle may be protected by Treg-mediated bystander suppression acting locally on the APCs, which take up and present all particle-associated antigens (Thornton and Shevach, 2000). In contrast, proteins that rapidly dissociate from inhaled particles also would escape Treg-mediated bystander suppression and thus would maintain allergenic potential. However, the Th2-inducing factors relevant at this second checkpoint are still not fully understood but would depend on additional risk factors, such as known protein-intrinsic, environmental, or genetic parameters.

Our findings have important clinical implications since they highlight the need to induce allergen-specific Treg responses rather than rely on strategies aimed at activating the existing Treg pool. To this end, our data suggest that the lung is a particularly promising antigen-targeting site for the induction of Treg responses (Soroosh et al., 2013), especially when considering the high Treg frequencies induced by minute quantities of inhaled antigens, estimated to be as little as 1 μg pollen protein per year (Platts-Mills and Woodfolk, 2011). Modification of the antigen formulation, such as stable integration into aerosolized particles, might represent a simple strategy to increase Treg induction upon lung targeting. Defining the physicochemical properties of inhaled antigens relevant for Treg activation or induction in vivo and establishing animal models mimicking human exposure to such environmental antigens will be important tasks for future studies. The ability to monitor antigen-specific Treg responses directly in humans, as demonstrated here, will facilitate subsequent translation into Treg-based therapeutic strategies.

STAR★METHODS

Detailed methods are provided in the online version of this paper and include the following:

- KEY RESOURCES TABLE
- CONTACT FOR REAGENT AND RESOURCE SHARING
- EXPERIMENTAL MODEL AND SUBJECT DETAILS

SUPPLEMENTAL INFORMATION

Supplemental Information includes five figures and can be found with this article online at http://dx.doi.org/10.1016/j.cell.2016.09.050.

AUTHOR CONTRIBUTIONS

P.B. designed the study, performed experiments, interpreted the data, and wrote the manuscript; F.H., U.S., and J.K. performed bioinformatics analyses; M.N. and N.B. performed TCR sequencing experiments; C.I. performed experiments; K.V. and B.S. performed TSDR analyses; S.B., M.M.H., G.G., C.A., O.K., A.A.B., F.F., and M. Wallner generated antigens; M.V., C.S., G.H., and M. Worm recruited study participants; M.A. interpreted data; and A.S. designed the study, interpreted the data, and wrote the manuscript. All authors provided discussion, participated in revising the manuscript, and agreed to the final version.

ACKNOWLEDGMENTS

We thank K. Rajewsky, U. Klein, S. Fillatreau, C. Romagnani, S. Rutz, A. Hamann, and C. Neumann for reviewing the manuscript; M. Knauel, M. Pötsch, A. Bittroff-Leben, G. Reifenberger, and T. Hohnstein for technical assistance; N. Heyen and R. Schaloske for graphical abstract design; the EUROIMMUN AG for providing recombinant grass proteins; and the DRFZ Flow Cytometry Core Facility and the BCRT Flow Cytometry Lab for cell sorting. This research was supported by the European Union 7th Framework Program as part of the project "The ONE Study" Grant Agreement HEALTH-F52010260687; Deutsche Forschungsgemeinschaft (DFG) grants SFB650 (TP5, 26), SFB/TR124 (TPA1, Z2), and SFB/TR 84 (TPA5); the Cystic Fibrosis Foundation (SCHEFF15G0); the German Federal Ministry of Education and Science (BMBF) - Project InfectControl 2020 (Fkz 03ZZ0802A, Fkz 03ZZ0813A "ART4Fun"), Grant "e:Med" (Fkz 01ZX1312A); and the priority program of the University of Salzburg "Allergy-Cancer-BioNano" Research Center. M.V., J.K., and M.A. are employees of Miltenyi Biotec. A.S. is a consultant for Miltenyi Biotec.

Received: May 27, 2016
Revised: August 11, 2016
Accepted: September 23, 2016
Published: October 20, 2016

REFERENCES

Bacher, P., and Scheffold, A. (2015). New technologies for monitoring human antigen-specific T cells and regulatory T cells by flow-cytometry. Curr. Opin. Pharmacol. *23*, 17–24.

Bacher, P., Schink, C., Teutschbein, J., Kniemeyer, O., Assenmacher, M., Brakhage, A.A., and Scheffold, A. (2013). Antigen-reactive T cell enrichment for direct, high-resolution analysis of the human naive and memory Th cell repertoire. J. Immunol. *190*, 3967–3976.

Bacher, P., Kniemeyer, O., Schönbrunn, A., Sawitzki, B., Assenmacher, M., Rietschel, E., Steinbach, A., Cornely, O.A., Brakhage, A.A., Thiel, A., and Scheffold, A. (2014a). Antigen-specific expansion of human regulatory T cells as a major tolerance mechanism against mucosal fungi. Mucosal Immunol. *7*, 916–928.

Bacher, P., Kniemeyer, O., Teutschbein, J., Thön, M., Vödisch, M., Wartenberg, D., Scharf, D.H., Koester-Eiserfunke, N., Schütte, M., Dübel, S., et al. (2014b). Identification of immunogenic antigens from Aspergillus fumigatus by direct multiparameter characterization of specific conventional and regulatory CD4+ T cells. J. Immunol. *193*, 3332–3343.

Baron, U., Floess, S., Wieczorek, G., Baumann, K., Grützkau, A., Dong, J., Thiel, A., Boeld, T.J., Hoffmann, P., Edinger, M., et al. (2007). DNA demethylation in the human FOXP3 locus discriminates regulatory T cells from activated FOXP3(+) conventional T cells. Eur. J. Immunol. *37*, 2378–2389.

Barzaghi, F., Passerini, L., and Bacchetta, R. (2012). Immune dysregulation, polyendocrinopathy, enteropathy, x-linked syndrome: a paradigm of immunodeficiency with autoimmunity. Front. Immunol. *3*, 211.

Bolstad, B.M., Irizarry, R.A., Astrand, M., and Speed, T.P. (2003). A comparison of normalization methods for high density oligonucleotide array data based on variance and bias. Bioinformatics *19*, 185–193.

Burastero, S.E., Paolucci, C., Breda, D., Longhi, R., Silvestri, M., Hammer, J., Protti, M.P., and Rossi, G.A. (2004). T-cell receptor-mediated cross-allergenicity. Int. Arch. Allergy Immunol. *135*, 296–305.

Cebula, A., Seweryn, M., Rempala, G.A., Pabla, S.S., McIndoe, R.A., Denning, T.L., Bry, L., Kraj, P., Kisielow, P., and Ignatowicz, L. (2013). Thymus-derived regulatory T cells contribute to tolerance to commensal microbiota. Nature *497*, 258–262.

Deifl, S., Zwicker, C., Vejvar, E., Kitzmüller, C., Gadermaier, G., Nagl, B., Vrtala, S., Briza, P., Zlabinger, G.J., Jahn-Schmid, B., et al. (2014). Glutathione-S-transferase: a minor allergen in birch pollen due to limited release from hydrated pollen. PLoS ONE *9*, e109075.

Duan, W., So, T., Mehta, A.K., Choi, H., and Croft, M. (2011). Inducible CD4+LAP+Foxp3- regulatory T cells suppress allergic inflammation. J. Immunol. *187*, 6499–6507.

Duhen, T., Duhen, R., Lanzavecchia, A., Sallusto, F., and Campbell, D.J. (2012). Functionally distinct subsets of human FOXP3+ Treg cells that phenotypically mirror effector Th cells. Blood *119*, 4430–4440.

Dziubianau, M., Hecht, J., Kuchenbecker, L., Sattler, A., Stervbo, U., Rödelsperger, C., Nickel, P., Neumann, A.U., Robinson, P.N., Mundlos, S., et al. (2013). TCR repertoire analysis by next generation sequencing allows complex differential diagnosis of T cell-related pathology. Am. J. Transplant. *13*, 2842–2854.

Ebinuma, H., Nakamoto, N., Li, Y., Price, D.A., Gostick, E., Levine, B.L., Tobias, J., Kwok, W.W., and Chang, K.M. (2008). Identification and in vitro expansion of functional antigen-specific CD25+ FoxP3+ regulatory T cells in hepatitis C virus infection. J. Virol. *82*, 5043–5053.

Ferreira, F., Engel, E., Briza, P., Richter, K., Ebner, C., and Breitenbach, M. (1999). Characterization of recombinant Bet v 4, a birch pollen allergen with two EF-hand calcium-binding domains. Int. Arch. Allergy Immunol. *118*, 304–305.

Girtsman, T., Jaffar, Z., Ferrini, M., Shaw, P., and Roberts, K. (2010). Natural Foxp3(+) regulatory T cells inhibit Th2 polarization but are biased toward suppression of Th17-driven lung inflammation. J. Leukoc. Biol. *88*, 537–546.

Gratz, I.K., and Campbell, D.J. (2014). Organ-specific and memory treg cells: specificity, development, function, and maintenance. Front. Immunol. *5*, 333.

Hsieh, C.S., Liang, Y., Tyznik, A.J., Self, S.G., Liggitt, D., and Rudensky, A.Y. (2004). Recognition of the peripheral self by naturally arising CD25+ CD4+ T cell receptors. Immunity *21*, 267–277.

Jin, H.S., Park, Y., Elly, C., and Liu, Y.C. (2013). Itch expression by Treg cells controls Th2 inflammatory responses. J. Clin. Invest. *123*, 4923–4934.

Joller, N., Lozano, E., Burkett, P.R., Patel, B., Xiao, S., Zhu, C., Xia, J., Tan, T.G., Sefik, E., Yajnik, V., et al. (2014). Treg cells expressing the coinhibitory molecule TIGIT selectively inhibit proinflammatory Th1 and Th17 cell responses. Immunity *40*, 569–581.

Josefowicz, S.Z., Niec, R.E., Kim, H.Y., Treuting, P., Chinen, T., Zheng, Y., Umetsu, D.T., and Rudensky, A.Y. (2012). Extrathymically generated regulatory T cells control mucosal TH2 inflammation. Nature *482*, 395–399.

Kabat, A.M., Harrison, O.J., Riffelmacher, T., Moghaddam, A.E., Pearson, C.F., Laing, A., Abeler-Dörner, L., Forman, S.P., Grencis, R.K., Sattentau, Q., et al. (2016). The autophagy gene Atg16l1 differentially regulates Treg and TH2 cells to control intestinal inflammation. eLife *5*, e12444.

Kearley, J., Barker, J.E., Robinson, D.S., and Lloyd, C.M. (2005). Resolution of airway inflammation and hyperreactivity after in vivo transfer of CD4+CD25+ regulatory T cells is interleukin 10 dependent. J. Exp. Med. *202*, 1539–1547.

Kieback, E., Hilgenberg, E., Stervbo, U., Lampropoulou, V., Shen, P., Bunse, M., Jaimes, Y., Boudinot, P., Radbruch, A., Klemm, U., et al. (2016). Thymus-Derived Regulatory T Cells Are Positively Selected on Natural Self-Antigen through Cognate Interactions of High Functional Avidity. Immunity *44*, 1114–1126.

Kuchenbecker, L., Nienen, M., Hecht, J., Neumann, A.U., Babel, N., Reinert, K., and Robinson, P.N. (2015). IMSEQ–a fast and error aware approach to immunogenetic sequence analysis. Bioinformatics *31*, 2963–2971.

Lathrop, S.K., Bloom, S.M., Rao, S.M., Nutsch, K., Lio, C.W., Santacruz, N., Peterson, D.A., Stappenbeck, T.S., and Hsieh, C.S. (2011). Peripheral education of the immune system by colonic commensal microbiota. Nature *478*, 250–254.

Lee, L.N., Ronan, E.O., de Lara, C., Franken, K.L., Ottenhoff, T.H., Tchilian, E.Z., and Beverley, P.C. (2011). CXCR6 is a marker for protective antigen-specific cells in the lungs after intranasal immunization against Mycobacterium tuberculosis. Infect. Immun. *79*, 3328–3337.

Legoux, F.P., Lim, J.B., Cauley, A.W., Dikiy, S., Ertelt, J., Mariani, T.J., Sparwasser, T., Way, S.S., and Moon, J.J. (2015). CD4+ T Cell Tolerance to Tissue-Restricted Self Antigens Is Mediated by Antigen-Specific Regulatory T Cells Rather Than Deletion. Immunity *43*, 896–908.

Levine, A.G., Arvey, A., Jin, W., and Rudensky, A.Y. (2014). Continuous requirement for the TCR in regulatory T cell function. Nat. Immunol. *15*, 1070–1078.

Ling, E.M., Smith, T., Nguyen, X.D., Pridgeon, C., Dallman, M., Arbery, J., Carr, V.A., and Robinson, D.S. (2004). Relation of CD4+CD25+ regulatory T-cell suppression of allergen-driven T-cell activation to atopic status and expression of allergic disease. Lancet *363*, 608–615.

Malhotra, D., Linehan, J.L., Dileepan, T., Lee, Y.J., Purtha, W.E., Lu, J.V., Nelson, R.W., Fife, B.T., Orr, H.T., Anderson, M.S., et al. (2016). Tolerance is established in polyclonal CD4(+) T cells by distinct mechanisms, according to self-peptide expression patterns. Nat. Immunol. *17*, 187–195.

Meiler, F., Zumkehr, J., Klunker, S., Rückert, B., Akdis, C.A., and Akdis, M. (2008). In vivo switch to IL-10-secreting T regulatory cells in high dose allergen exposure. J. Exp. Med. *205*, 2887–2898.

Mikhak, Z., Strassner, J.P., and Luster, A.D. (2013). Lung dendritic cells imprint T cell lung homing and promote lung immunity through the chemokine receptor CCR4. J. Exp. Med. *210*, 1855–1869.

Moon, J.J., Dash, P., Oguin, T.H., 3rd, McClaren, J.L., Chu, H.H., Thomas, P.G., and Jenkins, M.K. (2011). Quantitative impact of thymic selection on Foxp3+ and Foxp3- subsets of self-peptide/MHC class II-specific CD4+ T cells. Proc. Natl. Acad. Sci. USA *108*, 14602–14607.

Oksanen, J., Blanchet, F.G., Kindt, R., Legendre, P., Minchin, P.R., O'Hara, R.B., Simpson, G.L., Solymos, P., Henry, M., Stevens, H., et al. (2015). vegan: Community Ecology Package. R package version 23-2 https://cran.r-project.org/web/packages/vegan/index.html.

Palomares, O., Ruckert, B., Jartti, T., Kucuksezer, U.C., Puhakka, T., Gomez, E., Fahrner, H.B., Speiser, A., Jung, A., Kwok, W.W., et al. (2011). Induction and maintenance of allergen-specific FOXP3+ Treg cells in human tonsils as potential first-line organs of oral tolerance. J. Allergy Clin. Immunol. *129*, 510–520.

Platts-Mills, T.A., and Woodfolk, J.A. (2011). Allergens and their role in the allergic immune response. Immunol. Rev. *242*, 51–68.

Rényi, A. (1961). On measures of information and entropy. In Proceedings of the Berkley Symposium on Mathematical Statistics and Probability *1*, 547–561.

Ritchie, M.E., Phipson, B., Wu, D., Hu, Y., Law, C.W., Shi, W., and Smyth, G.K. (2015). limma powers differential expression analyses for RNA-sequencing and microarray studies. Nucleic Acids Res. *43*, e47.

Rowe, J.H., Ertelt, J.M., Xin, L., and Way, S.S. (2012). Pregnancy imprints regulatory memory that sustains anergy to fetal antigen. Nature *490*, 102–106.

Rudensky, A.Y. (2011). Regulatory T cells and Foxp3. Immunol. Rev. *241*, 260–268.

Sadras, V., and Bongiovanni, R. (2004). Use of Lorenz curves and Gini coefficients to assess yield inequality within paddocks. Field Crops Res. *90*, 303–310.

Sakaguchi, S., Yamaguchi, T., Nomura, T., and Ono, M. (2008). Regulatory T cells and immune tolerance. Cell *133*, 775–787.

Samstein, R.M., Josefowicz, S.Z., Arvey, A., Treuting, P.M., and Rudensky, A.Y. (2012). Extrathymic generation of regulatory T cells in placental mammals mitigates maternal-fetal conflict. Cell *150*, 29–38.

Schoenbrunn, A., Frentsch, M., Kohler, S., Keye, J., Dooms, H., Moewes, B., Dong, J., Loddenkemper, C., Sieper, J., Wu, P., et al. (2012). A converse 4-1BB and CD40 ligand expression pattern delineates activated regulatory T cells (Treg) and conventional T cells enabling direct isolation of alloantigen-reactive natural Foxp3+ Treg. J. Immunol. *189*, 5985–5994.

Shafiani, S., Dinh, C., Ertelt, J.M., Moguche, A.O., Siddiqui, I., Smigiel, K.S., Sharma, P., Campbell, D.J., Way, S.S., and Urdahl, K.B. (2013). Pathogen-specific Treg cells expand early during mycobacterium tuberculosis infection but are later eliminated in response to Interleukin-12. Immunity *38*, 1261–1270.

Smyth, G.K. (2004). Linear models and empirical bayes methods for assessing differential expression in microarray experiments. Stat. Appl. Genet. Mol. Biol. Published online February 12, 2004. http://dx.doi.org/10.2202/1544-6115.1027.

Soroosh, P., Doherty, T.A., Duan, W., Mehta, A.K., Choi, H., Adams, Y.F., Mikulski, Z., Khorram, N., Rosenthal, P., Broide, D.H., and Croft, M. (2013). Lung-resident tissue macrophages generate Foxp3+ regulatory T cells and promote airway tolerance. J. Exp. Med. *210*, 775–788.

Soyer, O.U., Akdis, M., Ring, J., Behrendt, H., Crameri, R., Lauener, R., and Akdis, C.A. (2013). Mechanisms of peripheral tolerance to allergens. Allergy *68*, 161–170.

Suffia, I.J., Reckling, S.K., Piccirillo, C.A., Goldszmid, R.S., and Belkaid, Y. (2006). Infected site-restricted Foxp3+ natural regulatory T cells are specific for microbial antigens. J. Exp. Med. *203*, 777–788.

Susani, M., Jertschin, P., Dolecek, C., Sperr, W.R., Valent, P., Ebner, C., Kraft, D., Valenta, R., and Scheiner, O. (1995). High level expression of birch pollen profilin (Bet v 2) in Escherichia coli: purification and characterization of the recombinant allergen. Biochem. Biophys. Res. Commun. *215*, 250–263.

Thomas, S.Y., Banerji, A., Medoff, B.D., Lilly, C.M., and Luster, A.D. (2007). Multiple chemokine receptors, including CCR6 and CXCR3, regulate antigen-induced T cell homing to the human asthmatic airway. J. Immunol. *179*, 1901–1912.

Thornton, A.M., and Shevach, E.M. (2000). Suppressor effector function of CD4+CD25+ immunoregulatory T cells is antigen nonspecific. J. Immunol. *164*, 183–190.

Traidl-Hoffmann, C., Jakob, T., and Behrendt, H. (2009). Determinants of allergenicity. J. Allergy Clin. Immunol. *123*, 558–566.

Ulges, A., Klein, M., Reuter, S., Gerlitzki, B., Hoffmann, M., Grebe, N., Staudt, V., Stergiou, N., Bohn, T., Brühl, T.J., et al. (2015). Protein kinase CK2 enables regulatory T cells to suppress excessive TH2 responses in vivo. Nat. Immunol. *16*, 267–275.

Vahl, J.C., Drees, C., Heger, K., Heink, S., Fischer, J.C., Nedjic, J., Ohkura, N., Morikawa, H., Poeck, H., Schallenberg, S., et al. (2014). Continuous T cell receptor signals maintain a functional regulatory T cell pool. Immunity *41*, 722–736.

Van Overtvelt, L., Wambre, E., Maillère, B., von Hofe, E., Louise, A., Balazuc, A.M., Bohle, B., Ebo, D., Leboulaire, C., Garcia, G., and Moingeon, P. (2008). Assessment of Bet v 1-specific CD4+ T cell responses in allergic and nonallergic individuals using MHC class II peptide tetramers. J. Immunol. *180*, 4514–4522.

Vukmanovic-Stejic, M., Sandhu, D., Sobande, T.O., Agius, E., Lacy, K.E., Riddell, N., Montez, S., Dintwe, O.B., Scriba, T.J., Breuer, J., et al. (2013). Varicella zoster-specific CD4+Foxp3+ T cells accumulate after cutaneous antigen challenge in humans. J. Immunol. *190*, 977–986.

Wallner, M., Hauser, M., Himly, M., Zaborsky, N., Mutschlechner, S., Harrer, A., Asam, C., Pichler, U., van Ree, R., Briza, P., et al. (2011). Reshaping the Bet v 1 fold modulates T(H) polarization. J. Allergy Clin. Immunol. *127*, 1571–1578.

Wambre, E., DeLong, J.H., James, E.A., LaFond, R.E., Robinson, D., and Kwok, W.W. (2012). Differentiation stage determines pathologic and protective allergen-specific CD4+ T-cell outcomes during specific immunotherapy. J. Allergy Clin. Immunol. *129*, 544–551.

Wan, Y.Y., and Flavell, R.A. (2007). Regulatory T-cell functions are subverted and converted owing to attenuated Foxp3 expression. Nature *445*, 766–770.

Yue, J.C., Clayton, M.K., and Lin, F.C. (2001). A nonparametric estimator of species overlap. Biometrics *57*, 743–749.

Zeileis, A. (2014). ineq: Measuring Inequality, Concentration, and Poverty. R package version 02-13 https://cran.r-project.org/web/packages/ineq/index.html.

Zhao, J., Zhao, J., Fett, C., Trandem, K., Fleming, E., and Perlman, S. (2011). IFN-γ- and IL-10-expressing virus epitope-specific Foxp3(+) T reg cells in the central nervous system during encephalomyelitis. J. Exp. Med. *208*, 1571–1577.

Zheng, Y., Chaudhry, A., Kas, A., deRoos, P., Kim, J.M., Chu, T.T., Corcoran, L., Treuting, P., Klein, U., and Rudensky, A.Y. (2009). Regulatory T-cell suppressor program co-opts transcription factor IRF4 to control T(H)2 responses. Nature *458*, 351–356.

Please cite this article in press as: Bacher et al., Regulatory T Cell Specificity Directs Tolerance versus Allergy against Aeroantigens in Humans, Cell (2016), http://dx.doi.org/10.1016/j.cell.2016.09.050

STAR★METHODS

KEY RESOURCES TABLE

REAGENT or RESOURCE	SOURCE	IDENTIFIER
Antibodies		
CD8-VioGreen (clone: BW135/80)	Miltenyi Biotec	Cat#130-096-902
CD14-VioGreen (clone: TÜK4)	Miltenyi Biotec	Cat#130-096-875
CD20-VioGreen (clone: LT20)	Miltenyi Biotec	Cat#130-096-904
CD4-APC-Vio770 (clone: Vit4)	Miltenyi Biotec	Cat#130-096-652
CD137-PE (clone: 4B4-1)	Miltenyi Biotec	Cat#130-093-475
CD137-VioBright FITC (clone: 4B4-1)	Miltenyi Biotec	Cat#130-104-516
CD45RO-APC (clone: UCHL1)	Miltenyi Biotec	Cat#130-095-460
CD45RO-PE-Vio770 (clone: UCHL1)	Miltenyi Biotec	Cat#130-096-739
CCR7-FITC (clone: REA108)	Miltenyi Biotec	Cat#130-099-172
CXCR3-PE-Vio770 (clone: REA232)	Miltenyi Biotec	Cat#130-101-381
CCR10-PE (clone: REA326)	Miltenyi Biotec	Cat#130-104-822
CLA-APC (clone: HECA-452)	Miltenyi Biotec	Cat#130-098-573
CD69-APC-Vio770 (clone: FN50)	Miltenyi Biotec	Cat#130-099-907
CD95-PE (clone: DX2)	Miltenyi Biotec	Cat#130-092-416
CD27-APC (clone: M-T271)	Miltenyi Biotec	Cat#130-093-186
CD31-PE (clone: AC128)	Miltenyi Biotec	Cat#130-092-653
CD45RA-APC (clone: T6D11)	Miltenyi Biotec	Cat#130-092-249
CRTH2-PE (clone: BM16)	Miltenyi Biotec	Cat#130-091-238
CD154-VioBlue (clone: 5C8)	Miltenyi Biotec	Cat#130-096-217
CD154-PE (clone: 5C8)	Miltenyi Biotec	Cat#130-092-289
CD154-APC (clone: 5C8)	Miltenyi Biotec	Cat# 130-092-290
TNF-α-PE-Vio770 (clone: cA2)	Miltenyi Biotec	Cat#130-096-755
IFN-γ-PE-Vio770 (clone 45-15)	Miltenyi Biotec	Cat#130-096-752
IL-17A-FITC (clone: CZ8-23G1)	Miltenyi Biotec	Cat#130-094-520
IL-17A-PE-Vio615 (clone: CZ8-23G1)	Miltenyi Biotec	Cat#130-107-145
IL-10-APC (clone: JES3-9D7)	Miltenyi Biotec	Cat#130-096-042
IL-5-Vio515 (clone: JES1-39D10)	Miltenyi Biotec	Cat#130-108-099
FOXP3-PE (clone: 3G3)	Miltenyi Biotec	Cat#130-093-014
Ki-67-PE (clone: REA183)	Miltenyi Biotec	Cat#130-100-289
CD152 (CTLA-4)-APC (clone: BNI3)	Miltenyi Biotec	Cat#130-097-682
HLA-A2-PE (clone: REA517)	Miltenyi Biotec	Cat#130-107-930
CD25-PE-Dazzle594 (clone: M-A251)	BioLegend	Cat#356126
CD127-BV605 (clone: A019D5)	BioLegend	Cat#351334
CD45RA-PE-Cy5 (clone: HI100)	BioLegend	Cat#304110
CCR6-BV605 (clone: G034E3)	BioLegend	Cat#353420
CRTH2-PerCP-Cy5.5 (clone: BM16)	BioLegend	Cat#350116
CCR4-BV421 (clone: L291H4)	BioLegend	Cat#359414
CCR4-PE-Dazzle594 (clone: L291H4)	BioLegend	Cat#359420
CCR8-PE (clone: L263G8)	BioLegend	Cat#360604
CXCR6-PE-Cy7 (clone: K041E5)	BioLegend	Cat#356012
CCR5-PE-Dazzle594 (clone: J418F1)	BioLegend	Cat#359126
CD11a-APC (clone: HI111)	BioLegend	Cat#301212
IL-4-BV605 (clone: MP4-25D2)	BioLegend	Cat#500828

(*Continued on next page*)

Continued

REAGENT or RESOURCE	SOURCE	IDENTIFIER
IFN-γ-PerCP-Cy5.5 (clone: 4S.B3)	BioLegend	Cat#502526
HELIOS-PacificBlue (clone: 22F6)	BioLegend	Cat#137220
IL-22-PerCP-eFluor710 (clone: 22URTI)	eBioscience	Cat#46-7229-42
CD154 MicroBead Kit, human	Miltenyi Biotec	Cat#130-092-658
CD137 MicroBead Kit, human	Miltenyi Biotec	Cat#130-093-476
CD28 pure – functional grade, human (clone: 15E8)	Miltenyi Biotec	Cat#130-093-375
CD40 pure – functional grade, human (clone: HB14)	Miltenyi Biotec	Cat#130-094-133
Anti-HLA-DR pure, human (clone: AC122)	Miltenyi Biotec	Cat#130-108-056
CD3 pure – functional grade, human (clone: OKT3)	Miltenyi Biotec	Cat#130-093-387
CD14 MicroBeads, human	Miltenyi Biotec	Cat#130-050-201
CD3 MicroBeads, human	Miltenyi Biotec	Cat#130-050-101
CD4+ T Cell Isolation Kit, human	Miltenyi Biotec	Cat#130-096-533
Chemicals, Peptides, and Recombinant Proteins		
Human AB Serum	GemCell, Gemini-Bioproducts	Cat#100-512
RPMI-1640 medium	GIBCO, Life Technologies	Cat#61870-044
TexMACS medium	Miltenyi Biotec	Cat#130-097-196
IL-2 (Proleukin)	Novartis	N/A
Rapamycin	Sigma Aldrich	Cat#R0395
Critical Commercial Assays		
MS Columns	Miltenyi Biotec	Cat#130-042-201
Viobility 405/520 Fixable Dye	Miltenyi Biotec	Cat#130-110-206
Treg Suppression Inspector	Miltenyi Biotec	Cat#130-092-909
CellTrace Violet Cell Proliferation Kit	Invitrogen, Molecular Probes	Cat#C34557
EpiTect Bisulfite Kit	QIAGEN	Cat#59104
FastStart Universal Probe Mastermix (ROX)	Roche Diagnostics	Cat#4913957001
SuperAmp lysis buffer	Miltenyi Biotec	Cat#130-092-562
Thermo Scientific terminal deoxynucleotidyl transferase	Thermo Scientific	Cat#EP0161
Expand Long Template PCR System DNA Pol Mix	Roche	Cat#11681842001
GE Healthcare Amersham CyDye Fluorescent Nucleotides	GE Healthcare	Cat#PA53021
Thermo Scientific Klenow Fragment	Thermo Scientific	Cat#EP0052
Gene Expression Hybridization Kit	Agilent Technologies	Cat#5188-5242
SurePrint G3 Human Gene Expression v2 8x60K Microarray Kit	Agilent Technologies	Cat#G4851B
Gene Expression Wash Buffer Kit	Agilent Technologies	Cat#5188-5327
illustra CyScribe GFX Purification Kit	GE Healthcare	Cat#27960602
Deposited Data		
Raw data files for the microarray analysis	NCBI GEO	GSE77081
Recombinant DNA		
Lambda DNA	New England Biolabs	Cat#N3011 S
Software and Algorithms		
R implementation of Yue-Clayton similarity index	This paper	N/A
R package ‘vegan’, version 2.3-2	(Oksanen et al., 2015)	https://cran.r-project.org/web/packages/vegan/index.html
R package ‘ineq’, version 0.2-13	(Zeileis, 2014)	https://cran.r-project.org/web/packages/ineq/index.html
R package ‘limma’	(Ritchie et al., 2015; Smyth, 2004)	https://bioconductor.org/packages/release/bioc/html/limma.html

(*Continued on next page*)

Continued

REAGENT or RESOURCE	SOURCE	IDENTIFIER
Agilent Feature Extraction Software FES 10.7.3.1		http://www.genomics.agilent.com/en/home.jsp
Other		
Egg whole (*Gallus gallus*)	Greer Laboratories	Cat#XPF271D3A2.5
Milk cow (*Bos taurus*)	Greer Laboratories	Cat#XPF395D3A2.5
Pork (*Sus scrofa*)	Greer Laboratories	Cat#XPF258D3A2.5
Tomato (*Solanum lycoperscium*)	Greer Laboratories	Cat#XPF225D3A5
Potato (*Solanum tuberosum*)	Greer Laboratories	Cat#XPF191D3A2.5
Wheat (*Triticum aestivum*)	Greer Laboratories	Cat#XPF235D3A2.5
Birch European White (*Betula pendula*)	Greer Laboratories	Cat#XP527D3A2.5
6 Grass-Mix (Ryegrass *Lolium perenne*, Timothy grass *Phleum pratense*, Orchard *Dactylis glomerata*, Kentucky Blue/June *Poa pratensis*, Meadow Fescue *Lolium pratensis*, Velvetgrass *Holcus lanatus)*	Greer Laboratories	Cat#XPGMX1A5
Mite *Dermatophagoides pteronyssinus*	Greer Laboratories	Cat#XPB82D3A2.5
Candida albicans	Greer Laboratories	Cat#XPM15D3A5
Staphylococcus aureus	InvivoGen	Cat#tlrl-hksa
Cytomegalovirus	Siemens Healthcare Diagnostics	Cat#OREA05
Tetanus Toxoid	Statens Serum Institute	N/A
Aspergillus fumigatus	ATCC	Cat#ATCC-46645
Escherichia coli	ATCC	Cat#ATCC-25922
Bacteroides fragilis	ATCC	Cat#ATCC-25285
Bacteroides thetaiotaomicron	ATCC	Cat#ATCC-29741
Clostridium leptum	DSMZ	Cat#DSM-753
Bacteroides ovatus	DSMZ	Cat#DSM-1896
Bacteroides vulgatus	DSMZ	Cat#DSM-1447
Influenza A (H1N1) MP1	Miltenyi Biotec	Cat#130-097-285
InfluenzaA (H1N1) MP2	Miltenyi Biotec	Cat#130-099-812
InfluenzaA (H1N1) NP	Miltenyi Biotec	Cat#130-097-278
A. fumigatus Asp f22	Miltenyi Biotec	Cat#130-099-776
A. fumigatus Gel1	Miltenyi Biotec	Cat#130-097-289
A. fumigatus Crf1	Miltenyi Biotec	Cat#130-096-775
A. fumigatus Asp f3 (pmp20)	Miltenyi Biotec	Cat#130-096-772
A. fumigatus Catalase B	Miltenyi Biotec	Cat#130-097-291
A. fumigatus Sod3 (SOD)	Miltenyi Biotec	Cat#130-097-288
A. fumigatus Shm2 (SHMT)	Miltenyi Biotec	Cat#130-097-290
A. fumigatus CcpA	recombinantly generated	(Bacher et al., 2014b)
A. fumigatus Scw4	recombinantly generated	(Bacher et al., 2014b)
A. fumigatus GliT	recombinantly generated	(Bacher et al., 2014b)
A. fumigatus Pst-1	recombinantly generated	(Bacher et al., 2014b)
A. fumigatus Asp f2	recombinantly generated	(Bacher et al., 2014b)
A. fumigatus CpcB	recombinantly generated	(Bacher et al., 2014b)
A. fumigatus TpiA	recombinantly generated	(Bacher et al., 2014b)
A. fumigatus Fg-gap	recombinantly generated	(Bacher et al., 2014b)
Birch Bet v1	recombinantly generated	(Wallner et al., 2011)
Birch Bet v2	recombinantly generated	(Susani et al., 1995)
Birch Bet v4	recombinantly generated	(Ferreira et al. 1999)
Birch Bet v6	recombinantly generated	This paper
Birch GST	recombinantly generated	(Deifl et al., 2014)

(*Continued on next page*)

Continued

REAGENT or RESOURCE	SOURCE	IDENTIFIER
Grass Phl p1	kindly provided by EUROIMMUN AG	N/A
Grass Phl p5	kindly provided by EUROIMMUN AG	N/A
Grass Phl p7	kindly provided by EUROIMMUN AG	N/A
Grass Phl p12	kindly provided by EUROIMMUN AG	N/A

CONTACT FOR REAGENT AND RESOURCE SHARING

Further information and requests for reagents may be directed to the corresponding author Alexander Scheffold (alexander.scheffold@charite.de).

EXPERIMENTAL MODEL AND SUBJECT DETAILS

Blood donors

Buffy coats or peripheral EDTA blood samples were obtained from the Institute for Transfusion Medicine, University Hospital Dortmund, Germany, the DRK Dresden, Germany, the Charité blood bank, Charité Berlin, Germany or from in-house volunteers. Peripheral EDTA blood samples from patients allergic to birch or *A. fumigatus*, were obtained from the Allergy Center or Cystic Fibrosis Center, Charité Berlin, Germany, respectively. Allergic donors were classified according history and antigen-specific Th2 cytokine production of $\geq$ 5%, which correlated with specific IgE levels (see Figures S5A and S5B). All blood donors gave informed consent (ethics committee Charité, EA1/290/13; EA1/096/14; EA1/094/15). PBMCs were freshly isolated on the day of blood donation by density gradient centrifugation (Biocoll; Biochrom, Berlin, Germany).

METHOD DETAILS

Antigen-reactive T cell enrichment

Antigen-reactive T cell enrichment (ARTE) was performed as previously described (Bacher et al., 2013, 2014a). In brief, 1-2 × 10^7 PBMCs were resuspended in 1 mL RPMI-1640 (GIBCO, Life Technologies, Darmstadt, Germany), supplemented with 5% (v/v) human AB-serum (GemCell, Gemini-Bioproducts, West Sacramento, CA, USA) in 12-well culture plates and stimulated for 7 hr in presence of 1 μg/ml CD40 and 1 μg/ml CD28 pure antibody (both Miltenyi Biotec, Bergisch Gladbach, Germany). 1 μg/ml Brefeldin A (Sigma Aldrich, Schnelldorf, Germany) was added for the last 2 hr. Cells were labeled with CD154-Biotin, CD137-PE, followed by anti-Biotin and anti-PE MicroBeads (CD154 and CD137 MicroBead Kit; both Miltenyi Biotec) and magnetically enriched by two sequential MS columns (Miltenyi Biotec). In some experiments CD137-VioBright FITC and antiFITC MicroBeads were used (both Miltenyi Biotec). Surface staining was performed on the first column, followed by fixation and intracellular staining on the second column. In some experiments 100 μg/ml antiHLA-DR pure antibody (Miltenyi Biotec; clone AC122) was added during stimulation. For stimulation and enrichment from cord blood samples, CD14+ monocytes were isolated from cord blood mononuclear cells (CBMCs) by positive selection with CD14 MicroBeads (Miltenyi Biotec) and cultivated for 2 days with antigen in X-Vivo15 (BioWhittaker/Lonza Walkersville, MD, USA), supplemented with 1000 IU/ml GM-CSF and 400 IU/ml IL-4 (both Miltenyi Biotec) to generate fastDCs. DCs were maturated for one day with 1000 IU/ml TNF-α, 1000 IU/ml IL1-β (both Miltenyi Biotec), 1 μg/ml PGE2 (Sigma Aldrich) and were used for stimulation of the autologous CD14- fraction. Enrichment of CD154+ and CD137+ T cells was performed as described above.

Frequencies of antigen-specific T cells were determined based on the total cell count of CD154+CD137- Tcons and CD137+CD154- Tregs after enrichment, normalized to the total number of CD4+ T cells applied on the column. For each stimulation, background enriched from the non-stimulated control was subtracted. For antigen-specific Tregs, a detection limit was defined as > 1.5 fold background cell number (non-stimulated control) and > 50 target cells per 10^5 stimulated input Treg after subtraction of the background.

Antigens

The following concentrations of antigens were used for stimulation (number of stimulated PBMC in parentheses): Birch, Grass both 100 μg/ml (1-2 × 10^7); Mite, *A. fumigatus*, *C. albicans* all 40 μg/ml (1-2 × 10^7); CMV, Tetanus both 10 μg/ml (1-2 × 10^7); *S. aureus* 10^8 heat killed cells/ml (1-2 × 10^7); Influenza mix from peptide pools MP1, MP2, NP all 0.6 nmol/ml (1-2 × 10^7); *E. coli*, *C. leptum*, *B. fragilis*, *B. ovatus*, *B. vulgatus*, *B. thetaiotaomicron* all 40 μg/ml (2 × 10^7); Egg, milk, pork, tomato, potato, wheat all 100 μg/ml (5 × 10^7); recombinant proteins Bet v1, Bet v2, Bet v4, Bet v6, GST, Phl p1, Phl p5, Phl p7, Phl p12, CcpA, Scw4, GliT, Pst-1, Asp f2, CpcB, TpiA, Fg-gap all 20 μg/ml (2 × 10^7); peptide pools Asp f22, Gel1, Crf1, Asp f3 (pmp20), CatB, Sod3 (SOD), Shm2 (SHMT) all 0.6 nmol/ml (2 × 10^7).

A. fumigatus mycelial lysate and recombinant proteins were generated as described (Bacher et al., 2014b). For generation of bacteria lysates, bacteria were grown on solid media (Columbia Blood Agar/ Biomérieux, Marcy l'Etoile France), harvested by scraping into 17.4 mL distilled water and lysed by addition of 0.4 mL NaOH (1N), 0.2 mL HCl (2N) and 2 mL 10 x PBS (pH 7.5). Lysis of cells was confirmed by microscopical analysis and by negative culture of lysates.

For generation of soluble and particle birch lysates, 180 mg whole birch pollen grains (Betula pendula; Allergon, Ängelholm, Sweden) were shaken for 5 hr in 1ml sterile water. After centrifugation for 10 min at 10.000 × g, the supernatant was taken as soluble lysate. The remaining pellet was disrupted using the GentleMACS device (Miltenyi Biotec) program RNA.01 (5 times). The lysate was centrifuged for 10 min at 400 × g to remove non-disrupted birch pollen grains and supernatant was taken as particle lysate.

Recombinant Bet v6 was produced in *E. coli* and purified from the soluble fraction of the bacterial lysate using a 5ml Q FF anion exchange chromatography column (GE Healthcare). The protein remained in the unbound fraction and was further purified by hydrophobic interaction chromatography with a 5 mL phenyl FF column (GE Healthcare).

Flow Cytometry

Cells were stained in different combinations of fluorochrome-conjugated antibodies (see Key Resources Table). Viobility 405/520 Fixable Dye (Miltenyi Biotec) was used to exclude dead cells. For intracellular staining cells were fixed and permeabilized with the Inside Stain Kit (Miltenyi Biotec). Staining for FOXP3, Ki-67, CTLA-4 and HELIOS was performed using the Foxp3 Staining buffer Set (Miltenyi Biotec). Data were acquired on a MACSQuant Analyzer 10 (Miltenyi Biotec), or LSR Fortessa (BD Bioscience, San Jose, CA, USA) and MACSQuantify (Miltenyi Biotec) or FlowJo (Treestar, Ashland, OR, USA) software was used for analysis.

In vitro T cell expansion and restimulation

Purified CD154+ Tcons or IL-4 producers in Figure S5 (IL-4 Secretion Assay Cell Enrichment and Detection Kit, Miltenyi Biotec) were expanded in presence of 1:100 irradiated feeder cells in TexMACS medium (Miltenyi Biotec), supplemented with 5% (v/v) human AB-serum (GemCell), 200 U/ml IL-2 (Proleukin®; Novartis, Nürnberg, Germany), and 100 IU/ml penicillin, 100 μg/ml streptomycin, 0.25 μg/ml amphotericin B (Antibiotic Antimycotic Solution, Sigma Aldrich) (from now on referred to as "expansion medium") at a density of 2.5 × 10^6 cells/cm^2. During expansion for 2-3 weeks, medium was replenished and cells were split as needed. Antigen-specific T cell clones were generated by single cell sorting of CD154+ T cells into 96-well round bottom plates with 1 × 10^5/well irradiated autologous feeder cells in expansion medium, supplemented with 10% AB-serum and additionally 20 μM β-Mercaptoethanol (GIBCO, Life Technologies), 2 mM glutamine and 30 ng/ml anti CD3 (OKT-3; Miltenyi Biotec). After 7 days, 100 μl medium was replenished and 1 × 10^5 irradiated feeder cells were added. For Treg cell lines, 1 × 10^4/well purified CD137+ cells were cultured in 96-well round-bottom plates in expansion medium, supplemented with 400 IU/ml IL-2 and additionally 30 nM rapamycin (Sigma Aldrich). Cells were expanded for 21 days, medium was replenished every 2-3 days.

For restimulation, fastDCs were generated from autologous CD14+ MACS isolated monocytes (CD14 MicroBeads; Miltenyi Biotec) by cultivation in X-Vivo15 medium (BioWhittaker/Lonza), supplemented with 1000 IU/ml GM-CSF and 400 IU/ml IL-4 (both Miltenyi Biotec). Before restimulation expanded T cells were rested in RPMI-1640 + 5% human AB-serum for 2 days. 1 × 10^5 expanded T cells were restimulated in a ratio of 1:1 with antigen-loaded fastDCs in 384-well flat bottom plates for 7 hr, with 1 μg/ml Brefeldin A (Sigma Aldrich) added for the last 4 hr.

In vitro proliferation assay

Isolated CD4+ responder T cells (Tresps) ($CD4^+$ T cell Isolation Kit, Miltenyi Biotec) were labeled with the CellTrace Violet Cell Proliferation Kit (Invitrogen, Molecular Probes®, Eugene, OR, USA). 1 × 10^5 Tresps were co-cultured in different ratios with antigen-specific Tregs and 2 × 10^5 Treg-autologous CD3-depleted (CD3 MicroBeads; Miltenyi Biotec) PBMCs as APCs and inducer of an alloreaction. Tregs were either stimulated specifically with their antigen or polyclonal with anti-CD3/CD28 beads (Treg Suppression Inspector; Miltenyi Biotec). On day 6, dilution of proliferation dye was analyzed by flow cytometry. Tresps could be discriminated from Tregs and APCs by using donors with opposite HLA-A2 expression.

Gel electrophoresis

Protein lysates were separated on a 4%–20% Tris-Glycine Gel (Anamed, Groß-Bieberau, Germany) by SDS-PAGE. Proteins were visualized by staining with Imperial Protein Stain Reagent (Thermo Fisher Scientific, Waltham, MA, USA).

FOXP3 TSDR methylation analysis

0.5-1 × 10^4 antigen-specific CD154+ and CD137+ CD4+ T cells were FACS purified. Genomic DNA was isolated using the QIAamp DNA Mini Kit (QIAGEN, Hilden, Germany) and bisulfite treated (EpiTect, QIAGEN). Real time-PCR was performed in a final reaction volume of 20 μl containing 10 μl FastStart Universal Probe Master (ROX) (Roche Diagnostics, Mannheim, Germany), 50 ng/μl Lambda DNA (New England Biolabs, Frankfurt, Germany), 5 pmol/μl methylation or non-methylation specific probe, 30 pmol/μl methylation or non-methylation specific primers and 60 ng bisulfite-treated DNA or respective amount of plasmid standard. The samples were analyzed in triplicates on an ABI 7500 Cycler. Percent *FOXP3* TSDR content was calculated by dividing the non-methylated copy number by the total genomic *FOXP3* copy number.

TCR sequencing and data analysis

NGS-based TCR repertoire analysis

Genomic DNA was isolated from FACS purified 0.5-1 × 10^4 antigen-specific CD154+ and CD137+ CD4+ T cells using the AllPrep DNA/RNA Micro Kit (QIAGEN). Recombined TCR-β locus was amplified as previously described (Dziubianau et al., 2013). Sequencing library preparation with consequent sequencing was performed using Illumina MiSeq Technology at NGS core facility at Berlin Brandenburger Center for Regenerative Therapies, Berlin, Germany. Reads with an average quality score below 30 were excluded from the analysis. The remaining high quality reads were processed using IMSEQ (Kuchenbecker et al., 2015). Each clonotype was assigned an ID including Vβ - and Jβ-gene identity as well as CDR3 amino acid sequence. Equal clonotypes were clustered and further analyzed.

Data analysis

The similarity of two populations was determined by the Yue-Clayton similarity index (Yue et al., 2001), which considers the proportion of each sequence in each population. The index is given by:

$$S_{YC} = \frac{\sum_{i=1}^{n_{PQ}} p_i q_i}{\sum_{i=1}^{n_{PQ}} (p_i - q_i)^2 + \sum_{i=1}^{n_{PQ}} p_i q_i}$$

where n_{PQ} is the the total number of sequences in the two populations P and Q; p_i is the proportion of the i^{th} sequence in population P; q_i is the proportion of the i^{th} sequence in population Q. The index ranges from 0 to 1, where 0 is total dissimilarity and 1 is identical populations. Linear regression was analyzed on $\log_{10}$ transformed frequencies, only sequences shared between the two groups were used for calculation and only if the two groups shared more than four sequences.

Clonal diversities of the TCR-β repertoires were evaluated for the top 50 expanded clones using Rényi diversity profiles (Rényi, 1961):

$$H_\alpha = \ln\left(\sum_{i=1}^{n} p_i^\alpha\right)\frac{1}{1-\alpha}$$

where H_α is the entropy; n is the total number of unique sequences; p_i is the proportion of the i^{th} sequence and α a scaling parameter.

By varying the α parameter, different diversity indices are calculated, such as the logarithm to the reciprocal Simpson diversity index at $\alpha = 2$. At $\alpha = 1$ the Rényi diversity is approximated by the Shannon diversity index. At $\alpha = 0$ and $\alpha =$ infinite, the profiles provide the logarithm of richness and the logarithm of the reciprocal to the proportion of the most abundant sequence (Berger-Parker Index), respectively. This means that the sample with the highest value at $\alpha = 0$ has the highest richness, but that the lower value at $\alpha =$ infinite indicates higher proportion of the most abundant sequence. A sample with a profile that is overall higher than the profiles of other samples is more diverse. Conversely, if the profiles cross at one point no ranking in diversity can be performed.

The equality of the distribution of TCR-β sequences was calculated for the top 50 expanded clones using the Gini coefficient (Sadras and Bongiovanni, 2004):

$$G = \frac{\sum_{i=1}^{n}(2i - n - 1)x_i}{n\sum_{i=1}^{n} x_i}$$

where x_i is the abundance of the i^{th} sequence, ranked in ascending order according to abundance and n is the total number of unique sequences. The coefficient ranges from 0 to 1, where 0 is total equality, i.e., all clones have the same proportion and 1 is total inequality, i.e., a population dominated by a single clone.

Microarray analysis

Sample preparation

For the generation of amplified cDNA (SuperAmp Service, Miltenyi Biotec), 4000 FACS purified antigen-specific CD154+ and CD137+ CD4+ T cells were lysed in SuperAmp lysis buffer (Miltenyi Biotec), the mRNA was extracted using magnetic beads and transcribed into cDNA using tagged random and oligo(dT) primer. First strand cDNA was 5′ tagged using a terminal deoxynucleotidyl transferase (Fisher Scientific) and globally amplified (Expand Long Template PCR System DNA Pol Mix; Roche) using primer complementary to the tag sequence. 250 ng of purified PCR product was labeled with Cy3-dCTP (Fisher Scientific) in a Klenow Fragment reaction (10 U) (Fisher Scientific).

Hybridization of Agilent Whole Human Genome Oligo Microarrays

The hybridization was performed according to the "One-Color Microarray-Based Gene Expression Analysis" protocol (part number G4140-90040) using the Agilent Gene Expression Hybridization Kit (Agilent Technologies, Santa Clara, CA, USA). Briefly, 0.5 μg Cy3-labeled cDNAs were hybridized overnight to Agilent Whole Human Genome Oligo Microarrays 8x60K v2 (AMADID 039494; Agilent

Technologies) using Agilent's recommended hybridization chamber and oven. Subsequently, microarrays were washed using the Agilent Gene Expression Wash Buffer Kit (Agilent Technologies). Fluorescence signals of the hybridized Agilent Microarrays were detected using Agilent's Microarray Scanner System (Agilent Technologies) and summarized in FES output files.

Data analysis

The intensity data were background corrected, quantile normalized (Bolstad et al., 2003), and log2 transformed. Transcripts were considered detected in a group, if 50% or more of the samples had a detection p value ≤ 0.05. The log2-transformed fold changes were calculated, p values ≤ 0.05 for differential expression between the compared groups was considered significant. The comparison of Tcon and Treg was done pairwise. For the evaluation of differential expression between allergic and healthy controls, the signal of every sample was compared to the opposite group median.

QUANTIFICATION AND STATISTICAL ANALYSIS

Statistical parameters including the exact value of n, the definition of center, dispersion and precision measure and statistical significance are reported in the Figures and the Figure Legends. Statistical tests were performed with GraphPad PRISM software 6.0 (GraphPad Software, La Jolla, CA, USA) or R statistical environment. Statistical tests were selected based on appropriate assumptions with respect to data distribution and variance characteristics, p values < 0.05 were considered statistically significant. EC_{50} values were calculated from dose-response curves using PRISM, the bottom and top of the curve were defined as 0 and 100, respectively.

DATA AND SOFTWARE AVAILABILITY

Software

The TCR diversity analysis was performed using R, version 3.2.2. Rényi diversity profiles were calculated using the R package 'vegan', version 2.3-2 (Oksanen et al., 2015). The Gini coefficients were calculated using the R package 'ineq', version 0.2-13 (Zeileis, 2014). Our implementation of Yue-Clayton similarity index in R is available upon request.

For read out and process the microarray image files, the Agilent Feature Extraction Software (FES) FES 10.7.3.1 was used. Microarray data analysis was performed using R, version 3.2.1; Platform: i386-w64-mingw32/i386 (32-bit). p values for differential expression were calculated using the R package 'limma' (Ritchie et al., 2015; Smyth, 2004).

Data Resources

The accession number for the microarray data reported in this paper is GEO: GSE77081.

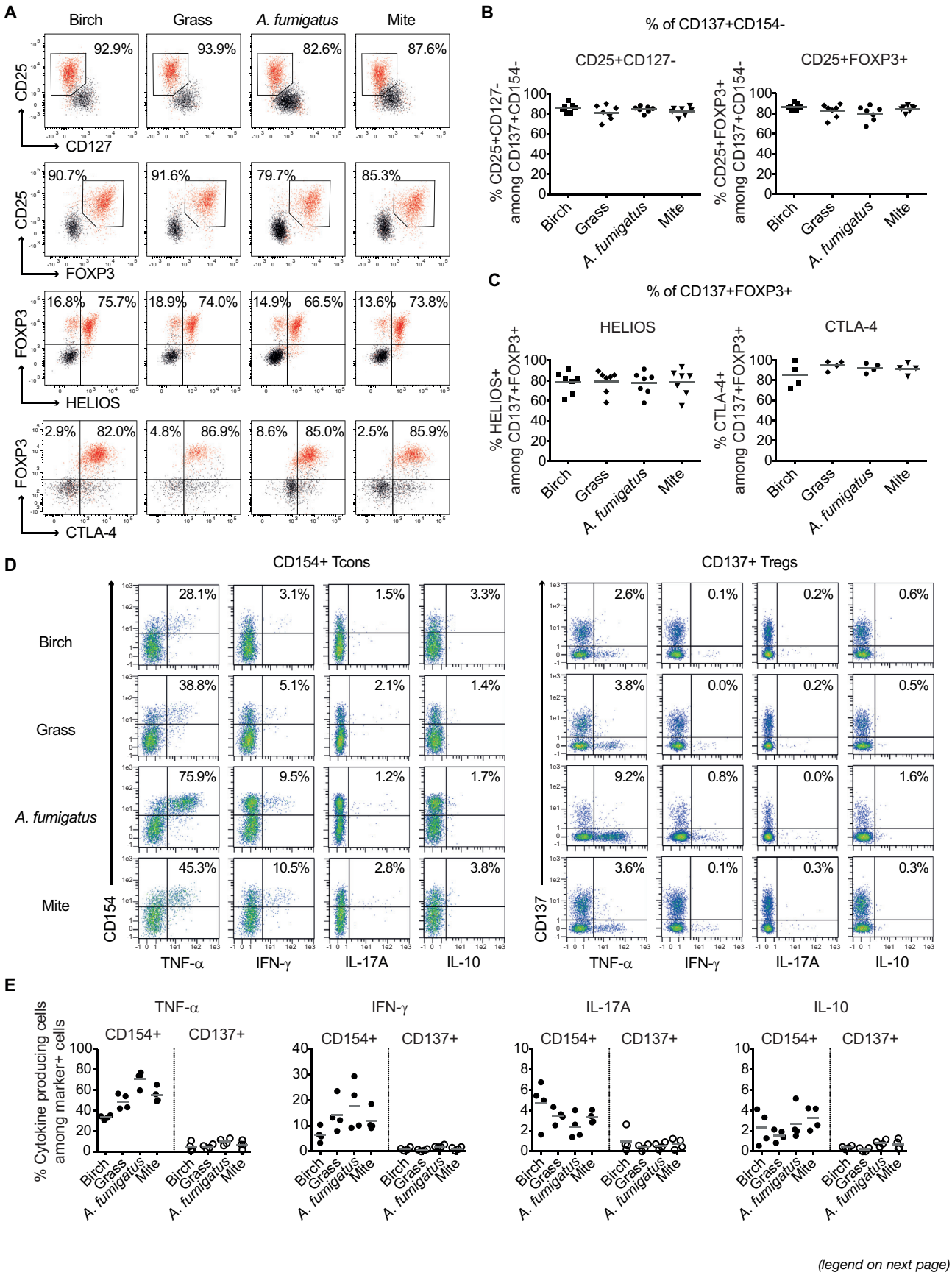

(legend on next page)

Figure S1. Antigen-Reactive CD137+CD4+ T Cells Express Typical Treg-Associated Markers, Lack Effector Cytokine Expression, and Show Suppressive Capacity, Related to Figure 1

(A) Representative dot plot examples showing expression of CD25, CD127, FOXP3, HELIOS and CTLA-4 on ex vivo enriched aeroantigen-specific CD154+ (black) and CD137+ (red) CD4+ T cells. Percentages of positive cells among CD137+CD4+ T cells are indicated.

(B and C) Statistical summary showing (B) the percentage of CD25+CD127- or CD25+FOXP3+ (n = 7) within aeroantigen-reactive CD137+CD154- cells or (C) the percentage of HELIOS+ (n = 7) or CTLA-4+ (n = 4) cells within CD137+FOXP3+ cells. Two independent experiments were performed.

(D and E) Ex vivo cytokine production of enriched aeroantigen-reactive T cells. (D) Representative dot plot examples. Cells were gated on CD4+ T cells and percentage of cytokine-expressing cells among CD154+ Tcon (left) and CD137+ Treg (right) is shown.

(E) Statistical summary (n = 4).

Each symbol in (B, C, E) represents one donor, horizontal bars indicate mean values.

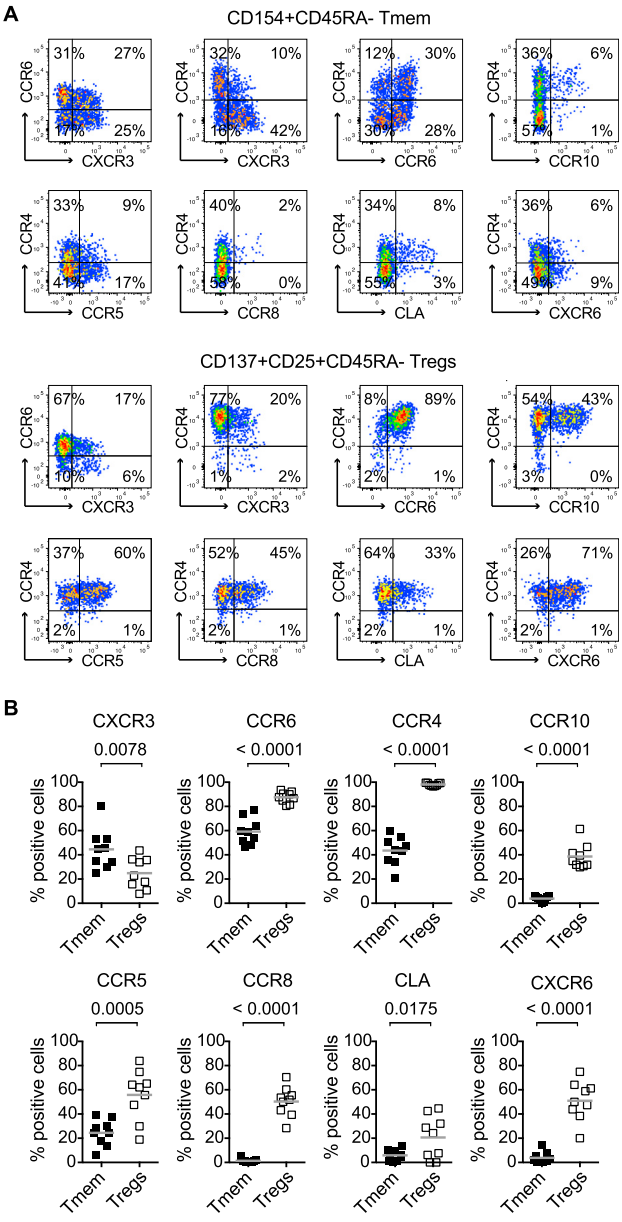

Figure S2. Tregs Specific for Aeroantigens Express Homing Markers Enabling Migration to the Lung Tissue, Related to Figure 1

(A and B) (A) Representative homing marker staining and (B) statistical summary of ex vivo enriched *A. fumigatus*-reactive CD154+CD45RA- Tmem and CD137+CD25+CD45RA- memory Tregs from healthy donors. Each symbol represents one donor (n = 9), horizontal bars indicate mean values. Statistical significance was determined by two-tailed paired t test. Three independent experiments were performed.

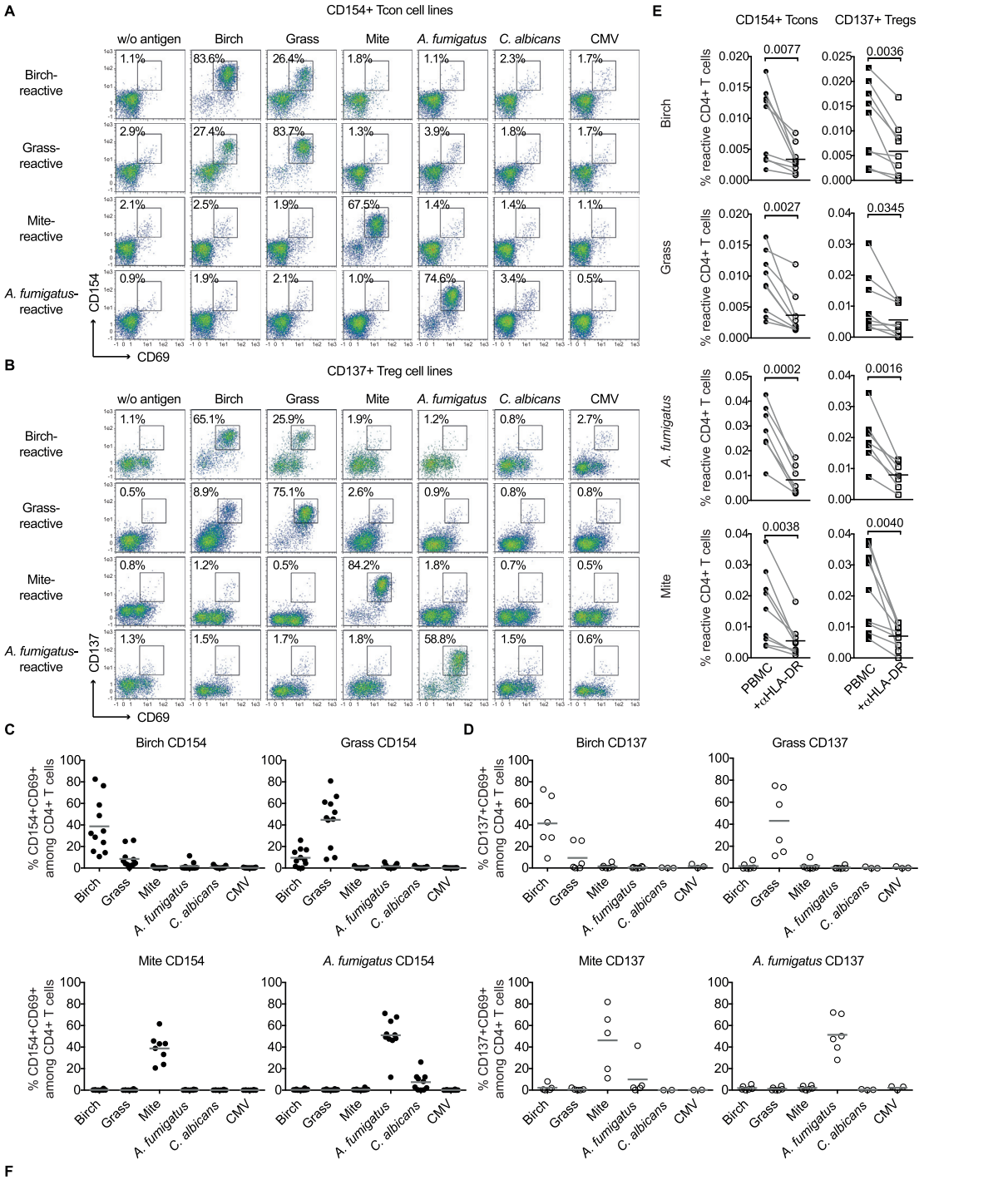

(legend on next page)

Figure S3. Specificity of CD154 and CD137 Induction, Related to Figure 1

(A–D) Aeroantigen-reactive T cell lines were expanded from isolated CD154+ Tcons and CD137+ Tregs, restimulated in presence of autologous APCs and analyzed for re-expression of activation markers. (A, B) Representative dot plot examples. Cells were gated on CD4+ T cells and percentage of CD154+CD69+ cells within antigen-reactive Tcon lines or CD137+CD69+ cells within antigen-reactive Treg lines is indicated. (C, D) Statistical summary (CD154: Mite n = 8, all others n = 11; CD137: Mite n = 5, all others n = 6). Two (CD137) or three (CD154) independent experiments were performed.

(E) PBMCs were ex vivo stimulated in presence or absence of an anti-HLA-DR pure antibody and frequencies of antigen-reactive CD154+ Tcons (left) and CD137+CD25+ Tregs (right) were determined using ARTE (*A. fumigatus* n = 7, all others n = 9). Four independent experiments were performed.

(F) Expanded aeroantigen-specific Treg lines were combined with autologous APCs and proliferation dye labeled allogeneic responder $CD4^+$ T cells (Tresps) in different Treg to Tresp ratios. Percentage of inhibition of Tresp proliferation is shown after antigen-specific restimulation (left) or polyclonal stimulation with CD3/CD28 beads (right). Graphs represent mean ± SEM of 3 donors for each antigen.

Each symbol in (C-E) represents one donor, horizontal bars indicate mean (C-E). Statistical differences two-tailed paired t test (E).

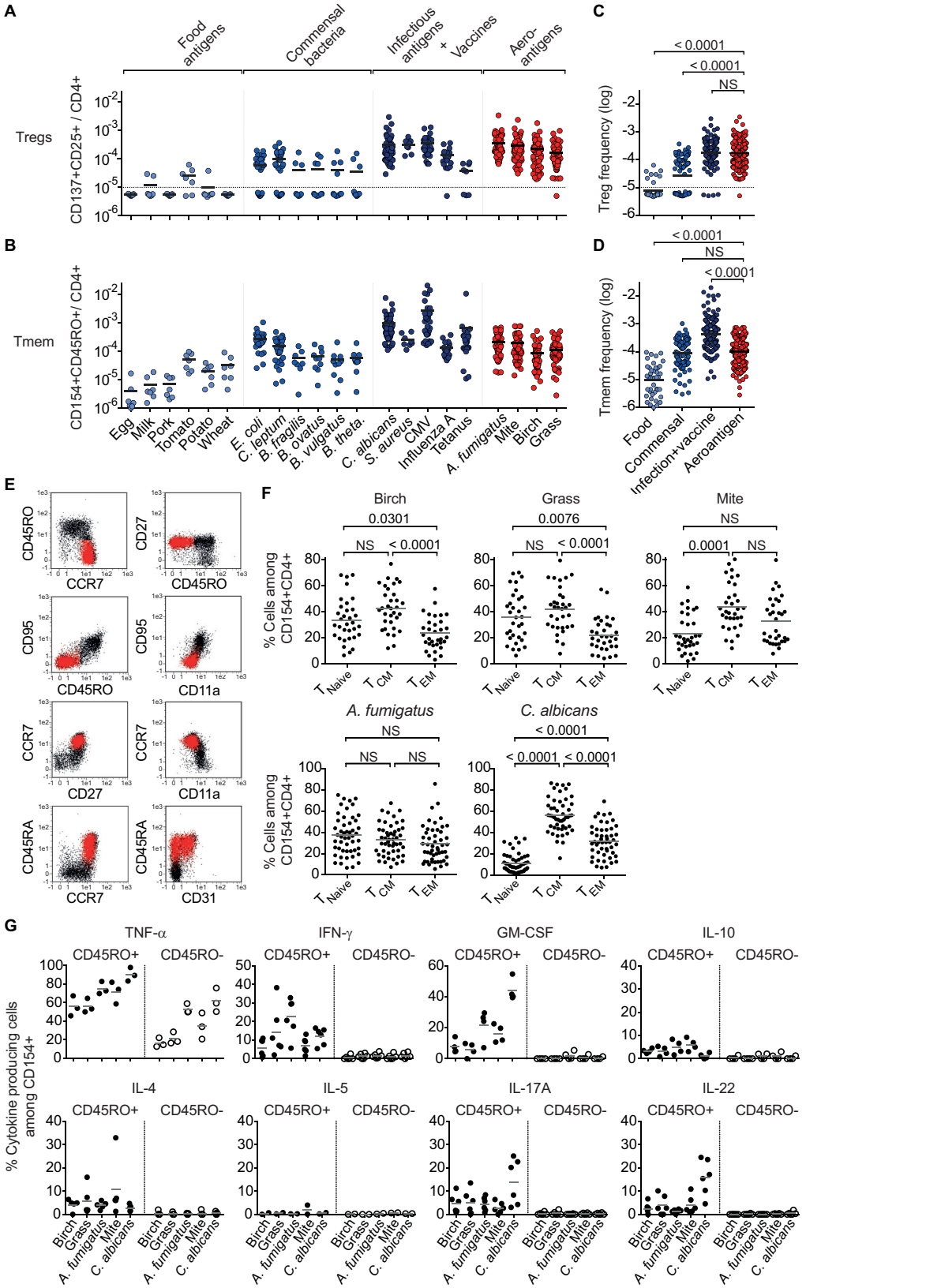

(legend on next page)

Figure S4. A Large Part of Tcons Specific for Aeroantigens Is Still in a Naive State, Related to Figure 2

(A and B) Frequencies of antigen-reactive CD137+ Tregs (A) or CD154+CD45RO+ Tmem (B). (Food: all n = 7; Commensal: *E. coli*, *C. leptum* n = 31, *B. ovatus* n = 8, all others n = 10; *C. albicans* n = 67; CMV n = 32; Influenza A n = 20; Tetanus Treg n = 8, Tmem n = 26; *S.aureus* n = 8; aeroantigens all n = 67). Values below the detection limit (dashed line) were assigned an arbitrary frequency value for graphical purposes.

(C and D) Frequencies from figure S4A and B were pooled according to the indicated groups and $\log_{10}$ transformed.

(E) Representative dot plot examples showing expression of phenotypic markers on *A. fumigatus*-reactive CD154+ T cells. Naive antigen-specific T cells colored in red were defined as CD154+CD45RO-CCR7+ and are shown as overlay with the total CD154+ population (black).

(F) Statistical summary showing the proportion of naive, central memory (Tcm) and effector memory (Tem) cells within CD154+CD4+ T cells (*A. fumigatus*, *C. albicans* n = 50; all others n = 33).

(G) Ex vivo cytokine production of antigen-reactive naive and memory T cells. Percentages of cytokine-expressing cells among CD154+CD45RO+ Tmem and CD154+CD45RO- Tnaive cells are shown (TNF-α n = 3, IFN-γ, IL-17, IL-22 n = 6; GM-CSF, IL-10 n = 4; IL-4 n = 5, IL-5 n = 2).

Each symbol in (A-D, F, G) represents one donor, horizontal bars indicate mean values. Statistical differences one-way ANOVA with Tukey post hoc test (C, D), two-tailed paired t test (F).

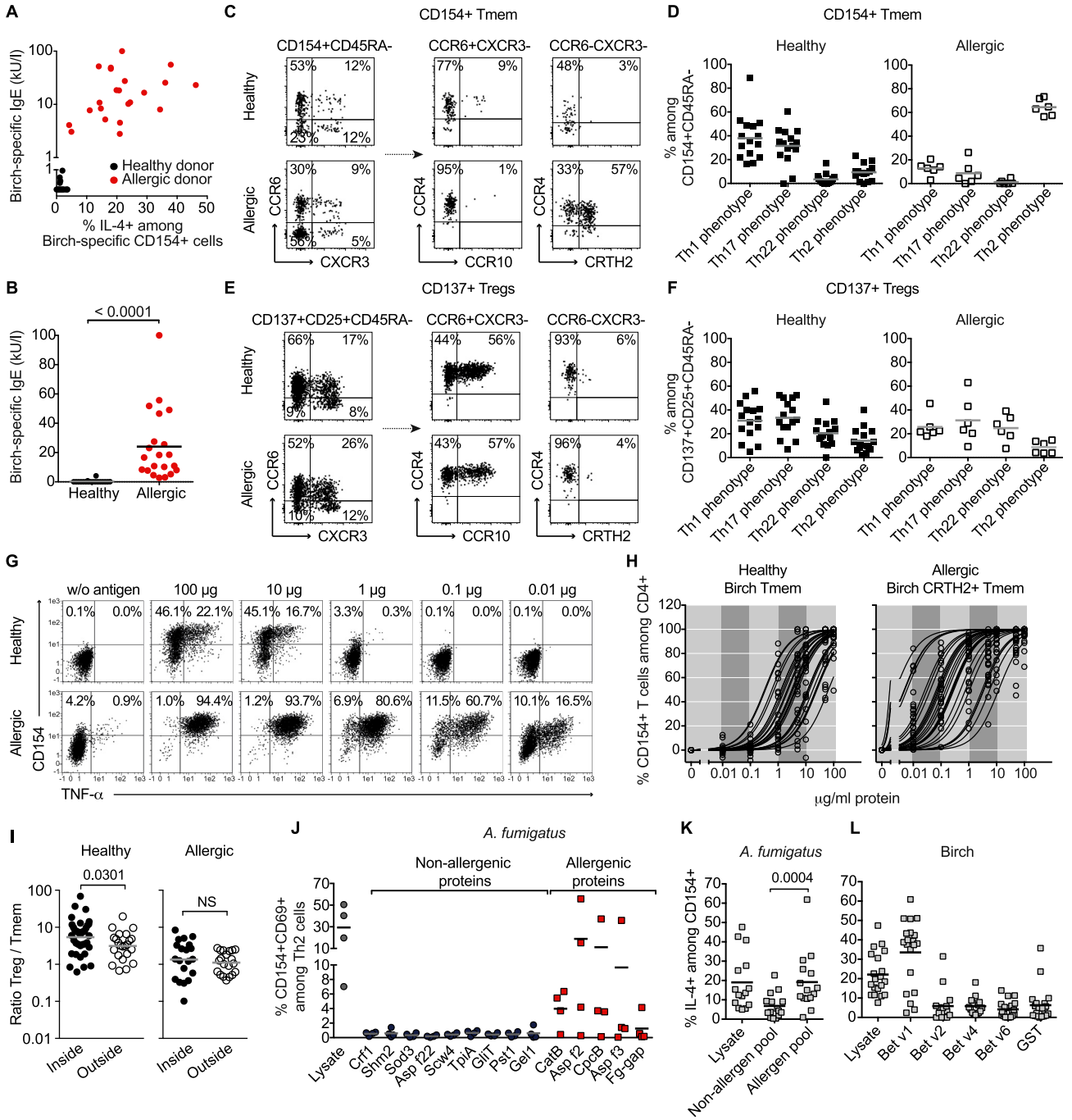

Figure S5. Phenotypical and Qualitative Alterations of Birch-Reactive Tmem, but Not Tregs, in Allergic Donors, Related to Figures 3, 4, and 5

(A) Ex vivo IL-4 production of birch stimulated CD154+ Tcons is plotted against birch-specific IgE levels. Allergic donors were defined according to antigen-specific Th2 cytokine production of ≥ 5%.

(B) Birch-specific IgE in healthy and allergic donors, defined according to (A).

(C–F) Flow cytometric analysis of CCR6, CXCR3, CCR4, CCR10 and CRTH2 expression on birch-reactive CD154+ Tmem (C, D) and CD137+ Tregs (E, F) from healthy (n = 15) and allergic donors (n = 6). T helper cell subsets were defined as Th1 = CXCR3+, Th17 = CXCR3-CCR6+CCR4+CCR10-, Th22 = CXCR3-CCR6+CCR4+CCR10+ and Th2 = CXCR3-CCR6-CCR4+ (Duhen et al., 2012). Each symbol represents one donor, the bars indicate mean values. Two (allergic donors) or four (healthy donors) independent experiments were performed.

(G) Representative dot plot examples for restimulation of expanded CD154+ Tmem clones from healthy and CD154+CRTH2+ Tmem clones from allergic donors. Cells were gated on CD4+ T cells and analyzed for CD154+ and TNF-α+ expression.

(legend continued on next page)

(H) Dose-response curves of single cell clones from birch-reactive CD154+ Tmem from healthy donors and CRTH2+ Tmem from allergic donors, restimulated with increasing antigen concentrations. Each line represents one T cell clone, summarized data from two healthy (n = 25) and two allergic donors (n = 28) are shown.

(I) Ratio of birch-specific memory Tregs/ Tmem inside (March-May) and outside (June-February) season (healthy inside n = 37, outside n = 23; allergic both n = 20).

(J) Th2 cell lines, generated from *A. fumigatus* allergic patients with cystic fibrosis (n = 4) and raised against a whole protein lysate from *A. fumigatus*, were restimulated with the indicated proteins. Proteins eliciting a response as determined by CD154 and CD69 induction, were defined as *A. fumigatus* allergenic proteins, whereas those not eliciting a response were defined as non-allergenic.

(K) Ex vivo stimulation of *A. fumigatus* allergic donors (n = 15) with pooled proteins, as defined in (J). Percentage of IL-4 production among CD154+ cells is shown.

(L) Ex vivo stimulation of birch allergic donors (n = 20) with the indicated single birch proteins. Percentage of IL-4 production among CD154+ cells is shown and demonstrates dominance of Bet v1, as major allergenic protein.

Each symbol in (A, B, D, F, I-L) represents one donor. Horizontal bars, mean (B, D, F, J-L), geometric mean (I). Statistical differences, two-tailed unpaired Mann-Whitney test and (B, I), two-tailed paired Wilcoxon test (K).